Technical Letter Report on Evaluation of Chemical Effects; Studies on Precipitates Used in Strainer Head Loss Testing

January 30, 2008

Prepared by
C. B. Bahn, K. E. Kasza, W. J. Shack, and K. Natesan
Argonne National Laboratory
Argonne, Illinois 60439

NRC Contract # JCN 3216
Program Manager: John Burke

Executive Summary

Argonne National Laboratory (ANL) performed additional testing related to GSI-191 chemical effects as part of technical support provided to the U.S. Nuclear Regulatory Commission. The purpose of these tests was to evaluate the properties of chemical precipitates that are used in sump strainer head loss testing by certain nuclear industry test vendors. Tests at ANL consisted of vertical loop head loss tests to evaluate precipitate filterability and bench-type tests that investigated precipitate characteristics such as particle size and settlement rate and solubility. Specific precipitates that were evaluated included aluminum oxyhydroxide (AlOOH) and sodium aluminum silicate (SAS) prepared according to the WCAP-16530-NP directions, along with precipitates formed from injection of sodium aluminate, calcium chloride, and sodium silicate according to the Control Components Inc. (CCI) test approach.

ANL had previously performed a vertical head loss loop with the WCAP AlOOH precipitate.[1] An additional head loss test using the WCAP AlOOH surrogate but at lower concentration was performed. The test confirmed that the surrogate is very effective in increasing the head loss across a glass fiber bed. The current result is consistent with that of the earlier ANL head loss test with the WCAP surrogate. In the ANL loop, only 1.5 ppm Al equivalent of surrogate (29.6 g/m^2) can completely plug a glass fiber bed. Tests with the WCAP sodium aluminum silicate (SAS) surrogate show that it is not quite as efficient as the WCAP AlOOH surrogate in increasing head loss. At low levels, the SAS surrogate tends to dissolve, especially in high purity water. However, in tap water, only 2 ppm Al equivalent SAS surrogate (172 g/m^2) is needed to generate a significant head loss. The particle sizes of the WCAP AlOOH surrogates range from 13-72 μm depending on the Al concentration in the mixing tank. For the same mixing concentration, the particle sizes of the SAS surrogate are larger than those of the AlOOH surrogate. The settling rates of the surrogates are strongly dependent on particle size, and the rates are reasonably consistent with those expected from Stokes Law or colloid aggregation models.

Surrogates were also created using the CCI procedure. Although aluminum and silicate are both added to the solution, the aluminum precipitate formed by the procedure probably consists primarily of aluminum hydroxide, since it would tend to form first in the CCI procedure. The characteristics of the precipitates strongly depend on whether in the solutions are made using high purity or ordinary tap water. In borated high purity water the aluminum hydroxide precipitates form extremely small particles with sizes ranging from 100-300 nm depending on the total Al concentration. These particles are much smaller than the WCAP surrogates. Literature results suggest that the sodium silicate that is present in the CCI procedure could act as a deflocculant for the aluminum hydroxide precipitates.[2,3] In borated tap water, the aluminum hydroxide precipitates are much larger than those formed in the solutions using high purity water, although they are still somewhat smaller than the WCAP surrogates. The effect of tap water on precipitate size may be attributable to the relatively high ionic strength of tap water due to dissolved cations like Ca^{2+}, Mg^{2+}, Na^{+} and the presence of anions like SO_4^{2-}, Cl^{-}, etc. The loop head loss tests showed that extremely small aluminum hydroxide precipitates (100-300 nm) produced using high purity water do not cause significant head loss while the 5.7 ppm Al equivalent of CCI-type precipitate made in tap water exhausted the pressure drop capacity of the ANL vertical loop.

Test Results

WCAP AlOOH Surrogate - Bench Top Test

Westinghouse report WCAP-16530-NP[4] provides a procedure for preparing surrogates for the $Al(OH)_3$* precipitates that can potentially form in sump solutions with high levels of dissolved Al following a loss-of-coolant-accident (LOCA). The procedure recognizes that the concentration during the precipitation process affects the size of the precipitate product and places limitations on the maximum concentrations in the mixing tanks. To verify that our bench top procedures produced results comparable to the larger scale mixing used by Westinghouse for preparing surrogates, settling rate tests for aluminum hydroxide surrogates were conducted. In our tests, 500 or 1000-mL Pyrex glass beakers were used as mixing tanks. The surrogate solutions were prepared using high-purity water and mixed for one hour using a magnetic stirrer. The relatively high concentrations of Na, Al, NO_3^- in these solutions dominate overall ionic strength and it is unlikely that there would be significant differences between WCAP surrogates prepared using high-purity or tap water. Three mixing tank concentrations were prepared with 2.2, 7.5, and 11 g of AlOOH per liter, respectively. Before starting the settling rate tests, the surrogate solutions were diluted to 2.2 g/L if needed. The settling rate tests were conducted in a 250-mL graduated mass cylinder. Figure 1 shows the normalized visible precipitate volumes as a function of time for different mixing tank concentrations; the ANL settling rate test results are shown along with the results from the Westinghouse report. Consistent with the results reported in the WCAP, for higher mixing tank concentrations, the precipitates settled more quickly. The differences between the ANL and the Westinghouse results are relatively small and can be attributed to the variability expected in this kind of experiment.

The particle size distributions of the AlOOH surrogates were measured by a laser granulometry technique (CILAS 1064 laser particle size analyzer). Figure 2a shows particle size distributions for two different 2.2 g/L AlOOH surrogate solutions. The median particle size is 12-14 μm. The particle size data appear to be reproducible. Figure 2b shows the effect of ultrasonic deflocculation. The median particle size was decreased from 12.5 to 7.5 μm by the ultrasonic deflocculation. Particle size after ultrasonic deflocculation is presumably a more intrinsic particle property while that before ultrasonic deflocculation could represent an agglomeration that may or may not hold together under shear flows. The flow rates in the sump are low, which suggests that the AlOOH surrogate is likely to stay in an agglomerated condition. Figure 3 shows the particle size distribution for a 11 g/L AlOOH surrogate. Since the upper size limit of the particle analyzer is 500 μm, particles larger than 500 μm could not be counted. The 11 g/L AlOOH surrogate appears to be quite agglomerated. The results after deflocculation are much closer to the results for the 2.2 g/L solution. As expected, the particle size is strongly dependent on the Al concentration in a mixing tank.

The particle size analysis results for WCAP AlOOH surrogate are consistent with the settling rate behavior as a function of Al concentration in mixing tanks shown in Figure 1, i.e., the larger particles settle faster.

*In this report, $Al(OH)_3$ is used a short–hand for a family of aluminum oxyhydroxides that could form in a variety of crystalline and amorphous forms.

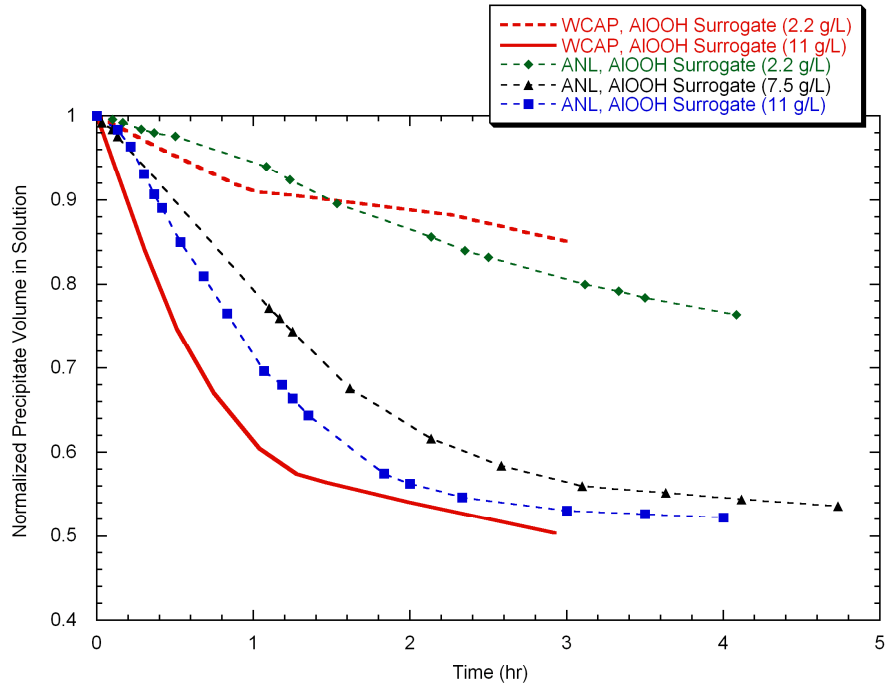

Figure 1. Comparison of WCAP and ANL test results for normalized visible precipitate volume variations in mixed AlOOH surrogates as a function time for different mixing tank concentrations.

Loop Head Loss Test – WCAP AlOOH

A head loss test was conducted using a WCAP AlOOH surrogate. The debris bed was formed on a perforated plate that has a 40% flow area and 1/8-in. holes with 3/16-in. staggered centers. The plate was mounted horizontally in a nominal 6-in. dia. transparent PVC plastic pipe vertical test section. The loop was filled with deionized water. Before the addition of the surrogate, 11.5 g of NUKON fiber was added to the loop. The NUKON fiber formed a bed on the perforated plate. This amount of material results in a bed of about 12 mm thickness under a screen approach velocity of 0.1 ft/s. The NUKON fibers were prepared by adding coarse shredded NUKON insulation to 1 liter of loop water in a household blender and blending the mixture for 11 sec in the high-ice crush mode. After this processing, another 1500 mL of loop water was added to the blended ingredients in a 3500-mL beaker and the 2500 mL mixture was magnetically stirred for 10 minutes at room temperature. The 2500 mL mixture was added to the tee port at the top of the loop in < 5 sec during which the mixture was stirred continuously. The fluid in the tee chamber was then stirred for another 2 minutes. The screen approach velocity was 0.1 ft/s during the building the NUKON bed and during all chemical additions after the bed was formed. The Al chemical additions were not started until the pressure drop across the NUKON bed had stabilized and the stabilized bed thickness measured. The loop water temperature was maintained at 80°F during the entire test.

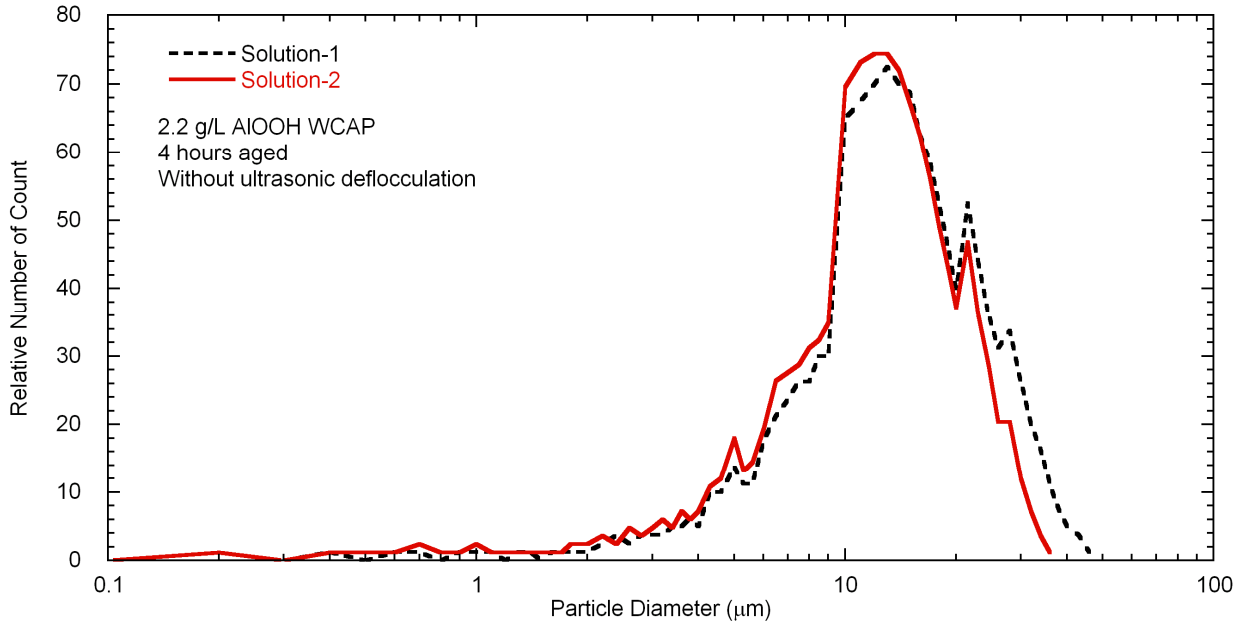

(a) Reproducibility of size distribution

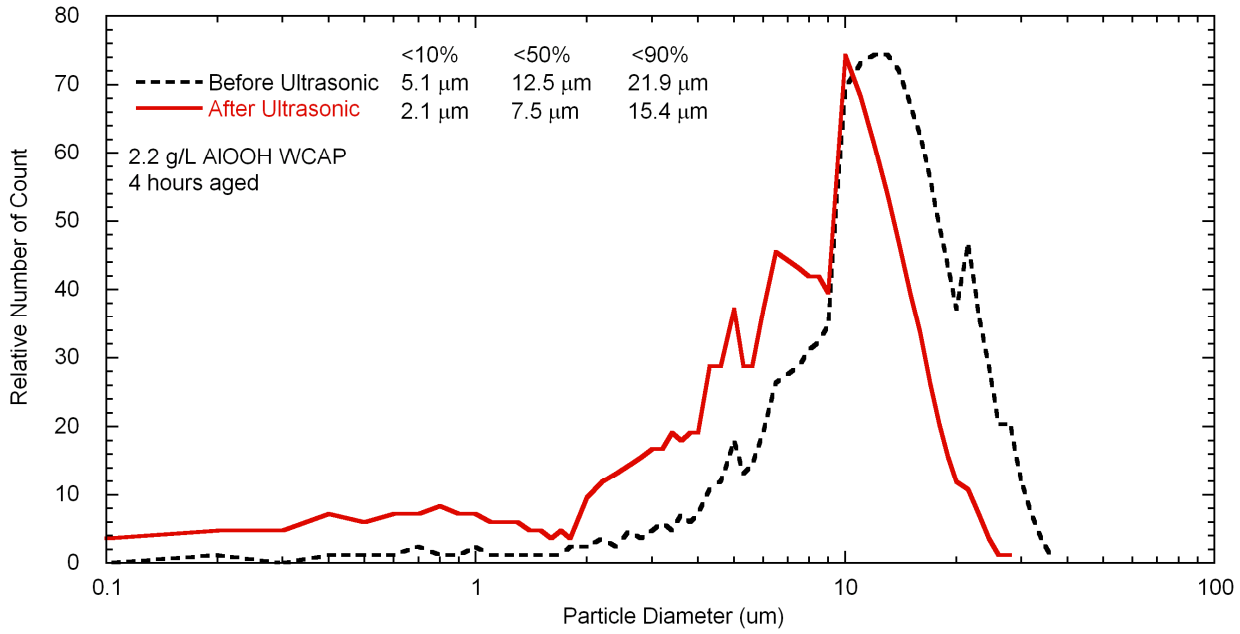

(b) Effect of ultrasonic deflocculation

Figure 2. Particle size distributions of WCAP AlOOH surrogates with a concentration of 2.2 g of AlOOH per liter (=1000 ppm Al); (a) data reproducibility and (b) effect of ultrasonic deflocculation.

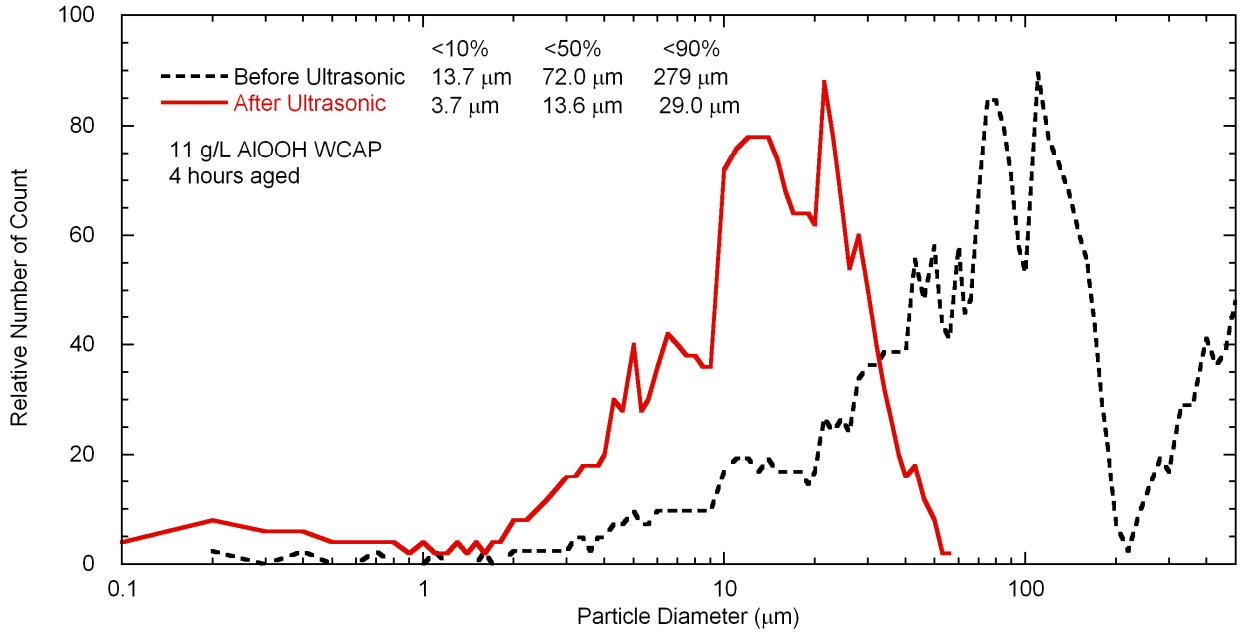

Figure 3. Particle size distributions of WCAP AlOOH surrogates with a concentration of 11 g of AlOOH per liter (5000 ppm Al) showing the effect of ultrasonic deflocculation.

Surrogate $Al(OH)_3$ product was prepared following the WCAP procedure. The AlOOH surrogate was prepared and kept well stirred in a 2000-mL Pyrex beaker. It was added to the loop through the tee port on the top of the loop in increments corresponding to the precipitation of 0.5 ppm Al from the loop volume of 118 liters. The total mass of precipitate added to the loop in the course of the test corresponded to the precipitation of 1.5 ppm Al from solution or a total of 394 mg of AlOOH. The effective flow diameter of the test section of 130 mm (5.125 in); thus the AlOOH load per unit screen area was 29.6 g/m^2.

Figure 4 shows the pressure drop and screen approach velocity time history during the test. The first 0.5 ppm equivalent Al surrogate addition caused a relatively small pressure-drop increase, but the second addition produced a significant increase in head loss. The third surrogate addition immediately resulted in a complete plugging of the NUKON bed. The screen approach velocity decreased with the increasing head loss because a recirculation pump was run in constant rpm mode. In previous ANL head loss tests[1], an initial 5 ppm Al addition as WCAP AlOOH surrogate caused a complete plugging of the bed. This head loss test result shows that only 1.5 ppm Al surrogate (or 29.6 g/m^2) can completely plug the NUKON bed in our test loop.

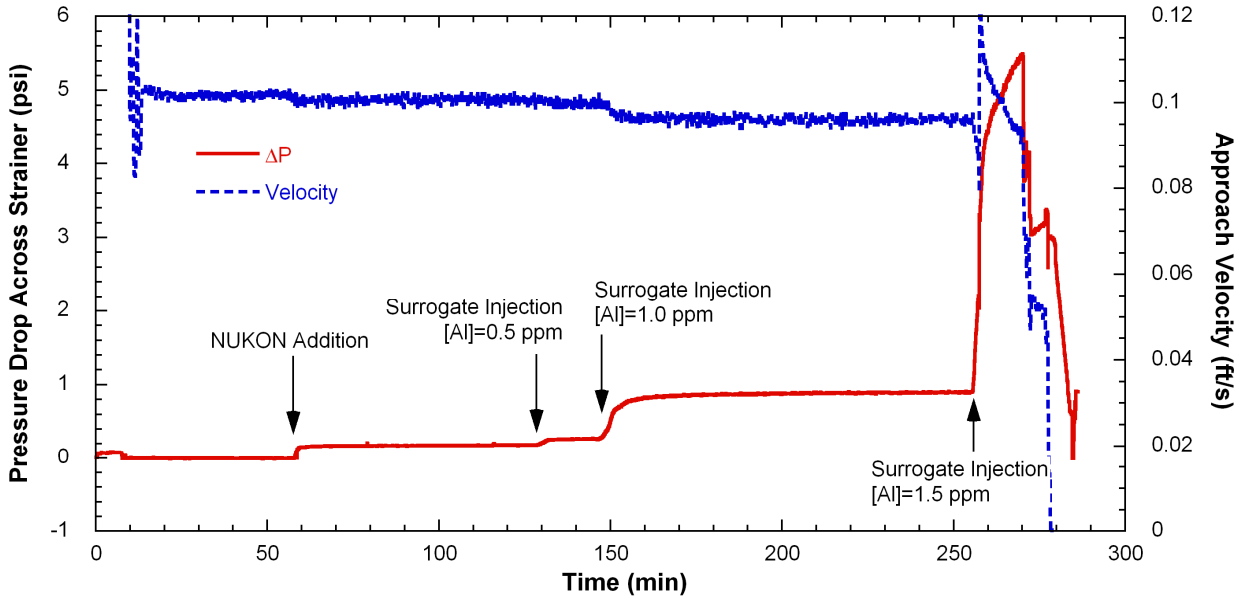

Figure 4. Pressure drop and screen approach velocity time history in a loop test using the WCAP aluminum hydroxide surrogates.

WCAP Sodium Aluminum Silicate Surrogate

Bench Top Tests – WCAP Sodium Aluminum Silicate

Sodium aluminum silicate (SAS, $NaAlSi_3O_8$) surrogate was prepared following the Westinghouse procedure. The surrogate was prepared from aluminum nitrate powder [$Al(NO_3)$-$9H_2O$, Alfa, 99.9 %] and sodium silicate powder [Na_4SiO_4, Alfa, 99.9%] added to high purity water. Two different mixing tank concentrations were used: 9.7 and 11 g of SAS per liter. The 9.7 g/L solution is equivalent to 1000 ppm Al concentration. The surrogate solution pH was strongly alkaline because of the excess sodium introduced by the sodium silicate.

Settling rate tests for the SAS surrogates were conducted. If necessary, before starting the settling rate tests, the surrogate solutions were diluted to get a concentration of 9.7 g/L. Figure 5 shows the normalized visible precipitate volume as a function of time. The Westinghouse report specifies the highest limit of mixing tank concentration as 11 g/L. As shown in Figure 5, the 11 g/L solution settles within one hour. One of the WCAP surrogate requirements is that normalized volume of precipitate in solution should be greater than 0.4 at the elapsed time of one hour. The experimental result for 11 g/L is close to the WCAP settlement limit of 0.4. This result confirms the choice of the highest mixing tank concentration as 11 g/L.

Settling rate tests for SAS surrogate were also conducted after the surrogate solution pH was adjusted to 8.6 using nitric acid, as shown in Figure 5. The settling behaviors of pH adjusted SAS surrogate solutions are quite different from the high pH solutions. This result suggests that the surrogate's physical and/or chemical characteristics like particle size or chemistry were altered by the pH change. The settling behaviors of pH adjusted SAS surrogate are very similar to those of AlOOH surrogate having 2.2 g/L concentration, as shown in

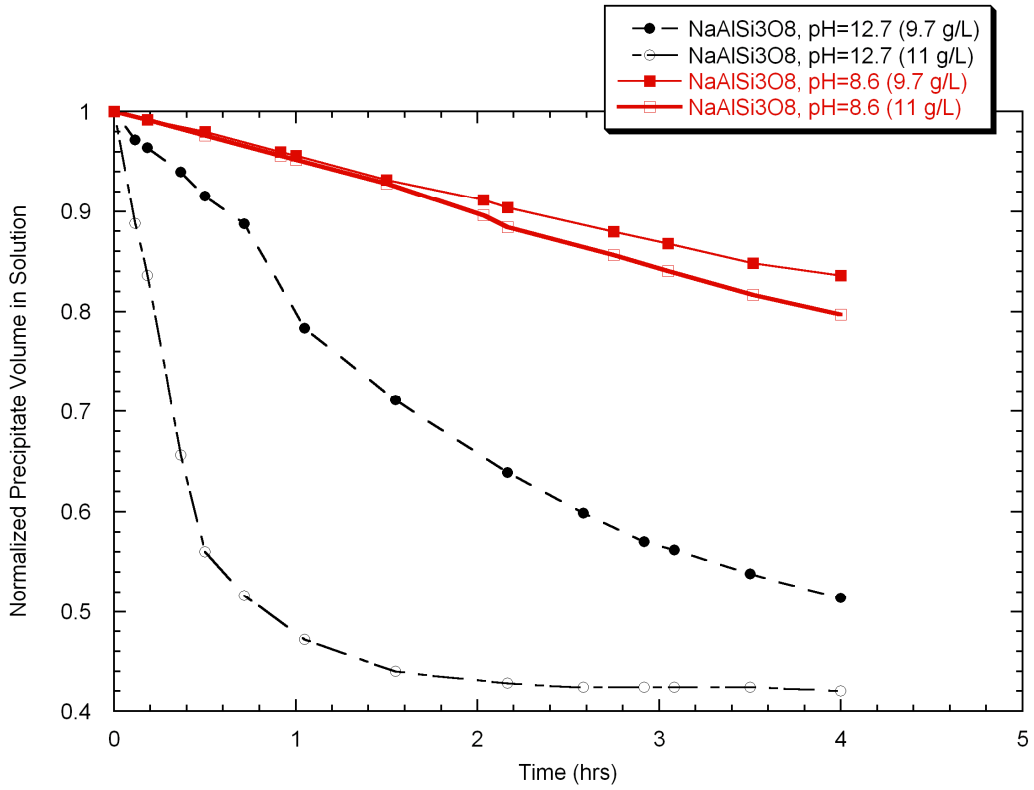

Figure 5. Normalized visible precipitate volume time history in mixed sodium aluminum silicate surrogate solution as a function of time and mixing tank concentration. In the low pH case it appears that the SAS has dissolved and AlOOH formed.

Figure 6, which is equivalent to 1000 ppm Al concentration. This suggests that the SAS dissolved and AlOOH formed because of low solubility of AlOOH at near neutral pH.

Particle sizes of the SAS surrogate were also measured by laser diffractometry, and the particle size distribution is shown in Fig. 7. The median particle size was 48 μm. The faster settling of SAS compared with AlOOH at the same Al concentration is consistent with the observed particle size differences. The particle size was also affected by ultrasonic deflocculation, which suggests that like the AlOOH surrogate, the SAS surrogate also tends to flocculate.

Dissolution tests in high purity and tap water were performed for the WCAP SAS surrogate to determine the stability of the surrogate. Visual observation showed that SAS surrogate additions to high purity water dissolved for Al levels less than 1.5 ppm, but at higher Al levels were not completely dissolved after 3 days. The SAS surrogate was much more stable in ANL tap water and only slight dissolution was observed. Filtered solution samples were analyzed using Inductively Coupled Plasma/Optical Emission Spectroscopy (ICP/OES). The analysis results are summarized in Table A1. The ICP analyses show that Al and Si concentrations in solution in high purity water increased according to the SAS surrogate injection but the Al and Si concentrations in solution in tap water did not significantly increase. The ICP results are consistent with visual observations of the solutions.

ICP analysis of ANL tap water revealed that it contains significant amounts of Ca (34 ppm), Mg (11 ppm), and Si (0.9 ppm). The preexisting ions in the tap water appear to affect the solubility of the SAS surrogate. It is noted that calcium silicate might also be formed in tap water when adding the SAS surrogate if any dissolution of the SAS occurs.

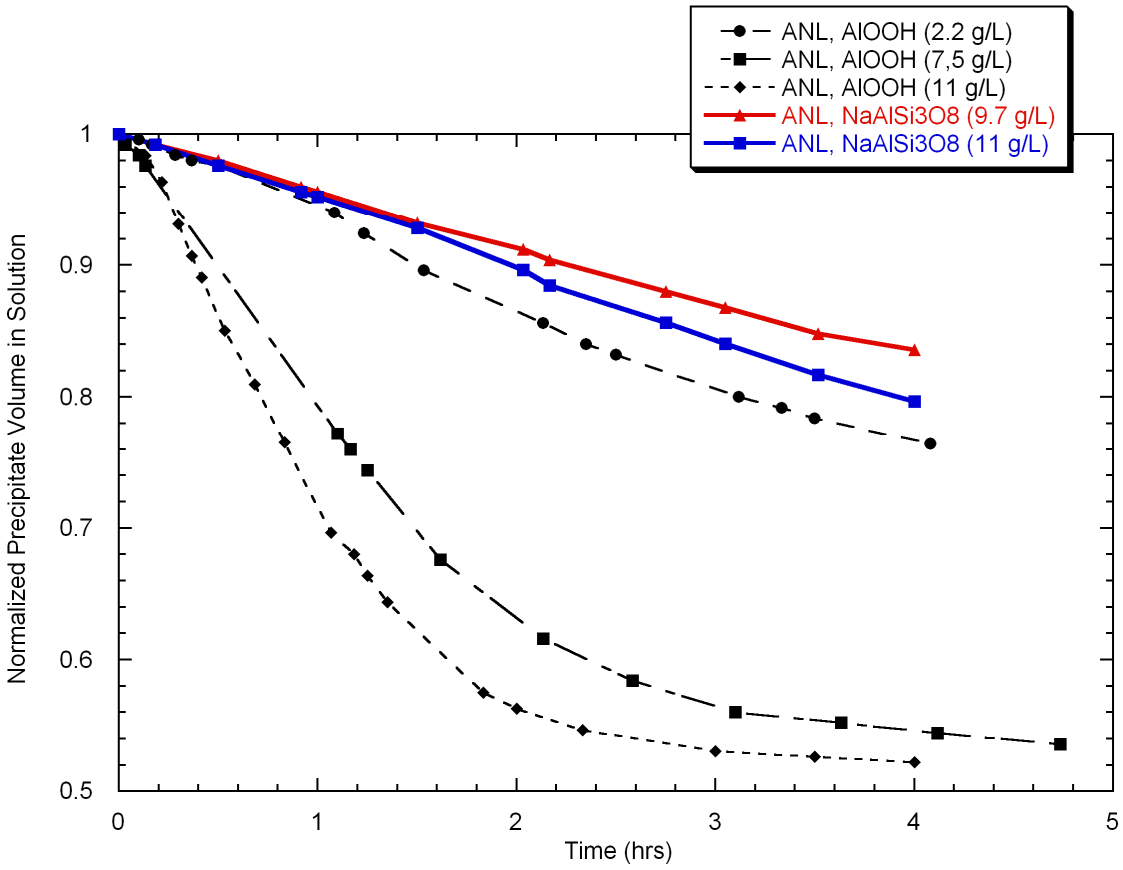

Figure 6. Normalized visible precipitate volume time history in mixed sodium aluminum silicate surrogate solution (pH=8.6) compared to those in mixed AlOOH surrogate solutions.

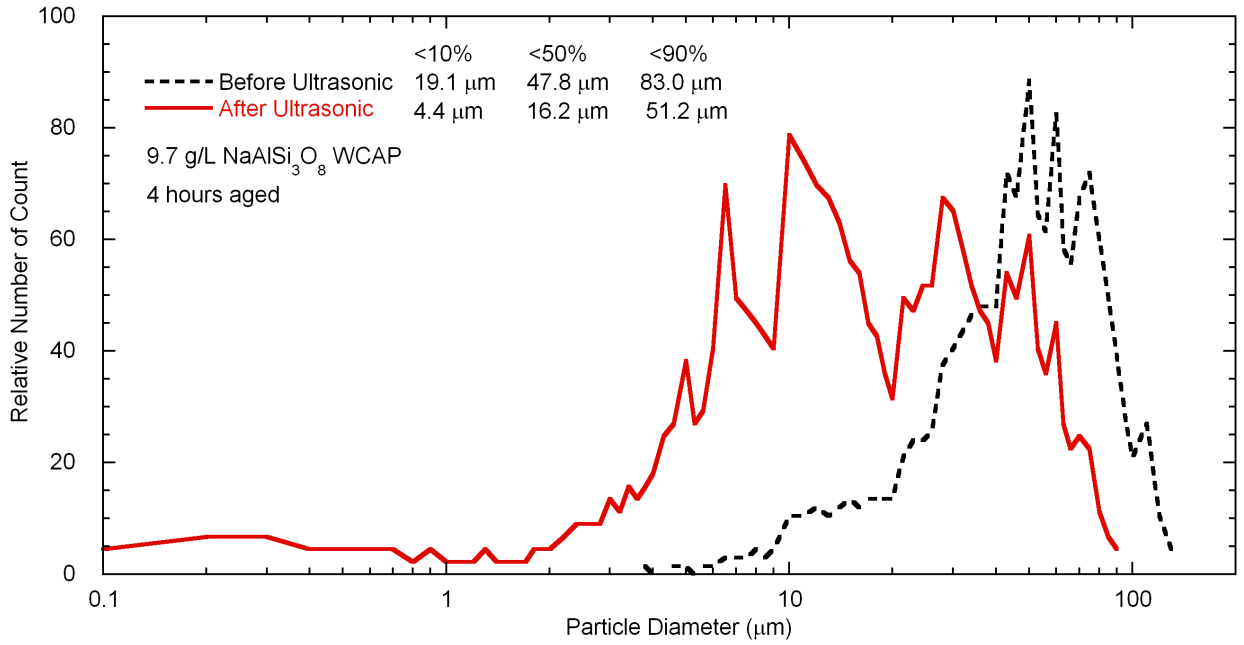

Figure 7. Particle size distributions of WCAP sodium aluminum silicate surrogates with a mixing concentration of 9.7 g of sodium aluminum silicate per liter (=1000 ppm Al) showing the effect of ultrasonic deflocculation.

Loop Head Loss Tests –WCAP Sodium Aluminum Silicate

The first loop test was run with high purity water. The loop was filled with high purity water, followed by NUKON addition, before addition of the surrogate similar to the AlOOH surrogate loop test. The temperature was maintained at 80°F. Figure 8 shows the pressure drop and screen approach velocity time history. On the first day, three boluses of the SAS surrogate were added into the loop. Each bolus was equivalent to a 0.5 ppm Al increase in the loop. For each addition, the response was always the same. The pressure drop across the bed rose to a peak value in the first minute or two and then over time would progressively decrease. During the test, there were two overnight rest periods without additions. Significant decreases in pressure drop occurred during the overnight periods, presumably due to dissolution of the SAS initially trapped in the bed.

No effort was taken as the pressure drop increased or decreased to maintain the screen approach velocity at 0.1 ft/s; it was allowed to fall in response to the increased pressure drop. Although the pressure drop peaked and then decreased after each addition, the NUKON bed retained some irreversible compression from the temporary peak in the pressure drop. Therefore, there was an increasing bed compression and pressure drop with each bolus even though there was pressure drop recovery due to the dissolution of SAS. The pressure drop decreases observed in the loop test are consistent with the observations of the bench top tests, in which SAS surrogate at these levels dissolves in high purity water.

At the end of the test, the loop pH was decreased by adding small doses of dilute nitric acid. Figure 8b shows the pressure drop time history for this portion of the test. No evidence of precipitation was observed for the first 8 boluses of acid, which reduced the loop water pH

down to 8.67. During this time the bed pressure drop continued to decline, at an even faster rate as the pH decreased, presumably due to further dissolution of SAS from the bed. However, immediately after adding the 9th bolus of acid, the pressure drop increased up to the loop capacity limit and the loop had to be shut down. The pressure drop increase after the final acid injection appears to be caused by the precipitation of aluminum hydroxide rather than SAS. It was noted previously that that difference in settling rate behaviors as a function of pH of the SAS surrogate solution, as shown in Figure 5, suggests that at a pH of ≈ 8.6 aluminum hydroxide, not SAS, is the most likely precipitate.

Because the bench top tests indicated that SAS is more stable in tap water than in high purity water, a second head loss test was conducted using tap water. The solution using tap water was more buffered, and the loop pH did not rise as high as in the previous SAS test with high purity water. Figure 9 shows the pressure drop and screen approach velocity time history in this loop test. The pressure drop increased more rapidly with addition of the surrogate than in the test with high purity water, although the pressure drop showed some decline overnight after a 1.5 ppm Al equivalent addition of SAS surrogate. After a 2.0 ppm Al equivalent addition of SAS surrogate the pressure drop did not decrease and remained stable over night, which suggests the loop water had reached the solubility limit of SAS. These results are consistent with the results of the bench top tests that showed less dissolution of SAS in tap water than in high purity water.

The WCAP SAS surrogate does not appear to be quite as efficient as the WCAP AlOOH surrogate in increasing head loss, and it is not quite as stable, especially in high purity water. However, only 2 ppm Al as SAS surrogate (total 2290 mg of SAS) in tap water caused significant head loss. The corresponding loading of SAS per unit screen area is 172.0 g/m^2.

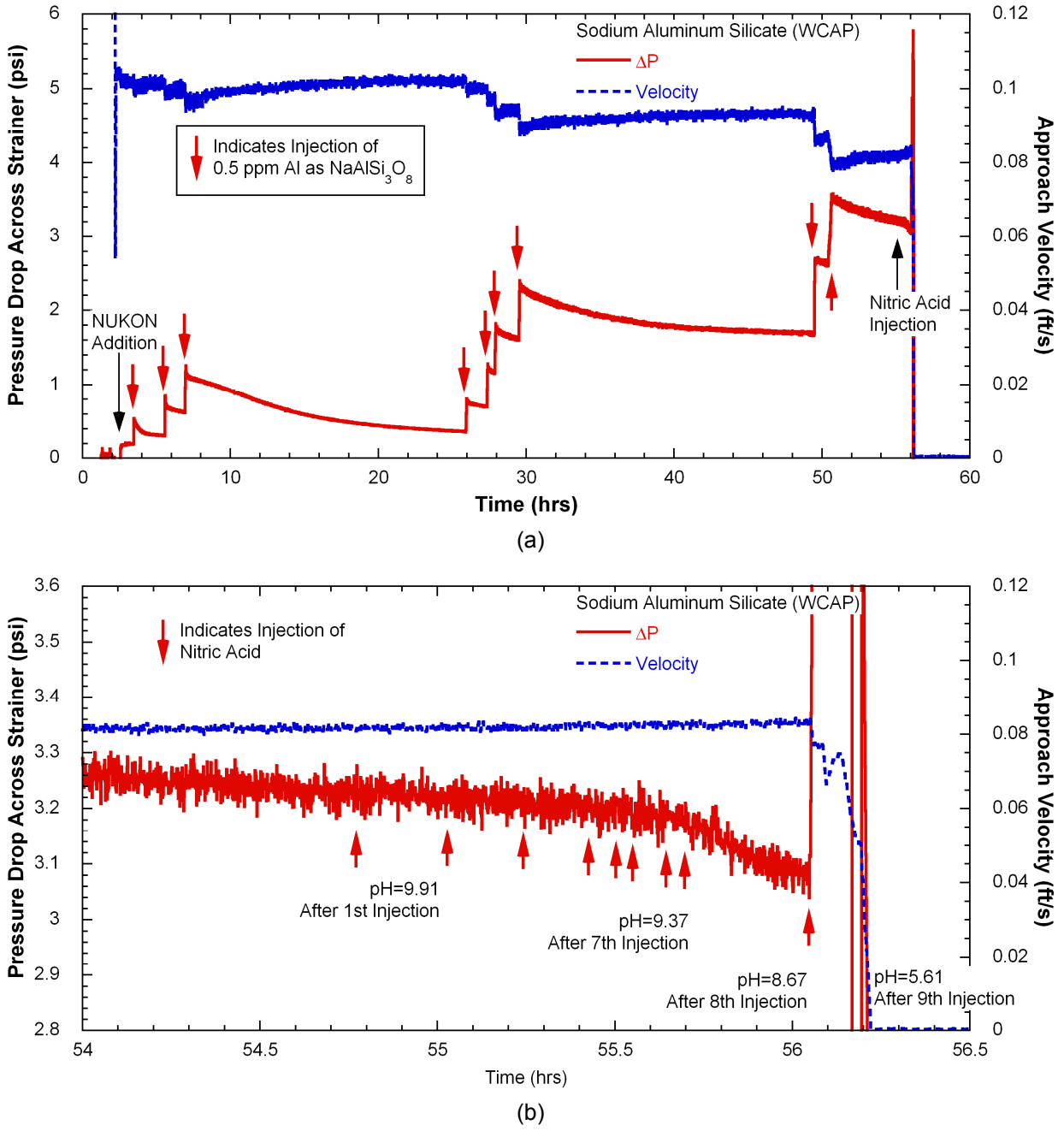

Figure 8. Pressure drop and screen approach velocity time history in loop test using the WCAP sodium aluminum silicate surrogates in high purity water showing (a) full time history and (b) history at nearly end.

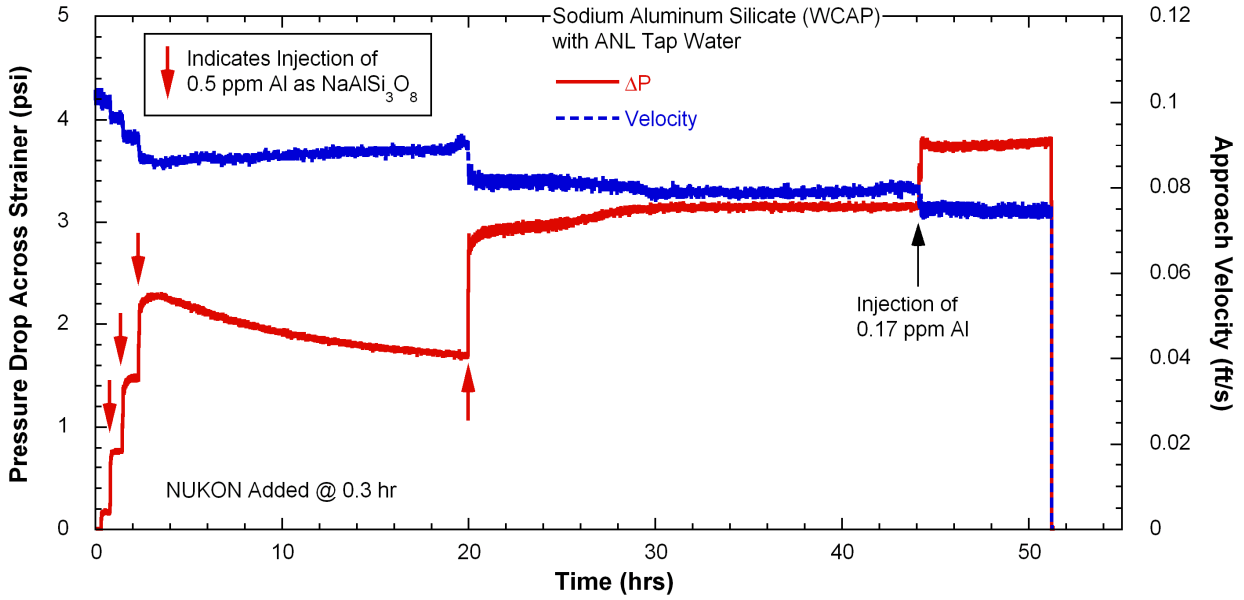

Figure 9. Pressure drop and screen approach velocity time history in loop test using the WCAP sodium aluminum silicate surrogate and ANL tap water.

Precipitates Formed by Direct Chemical Addition

Bench Top Tests

In some cases, procedures different from those described in the WCAP[4] have been used to make surrogates. A plant-specific surrogate preparation procedure developed by CCI was taken as the basis for testing. In the CCI approach, sodium aluminate is used as the source of Al, and the mixing concentrations are (at least nominally) much lower than in the WCAP procedure. The procedure also includes a wider range of chemicals, reflecting those determined in the plant, than are used to create the WCAP surrogate. For the tests performed here, the chemical makeup was patterned after a specific plant. The chemical concentrations chosen were as follows: 2500 ppm B, 115 ppm Al, 82 ppm Ca, and 670 ppm SiO_2 (=313 ppm Si).

In our initial studies, high purity water was used. In the CCI procedure, boric acid (H_3BO_3, Alfa) is added to the water, and then sodium aluminate ($NaAlO_2$, Alfa) solution is added. At this step an aluminum hydroxide precipitate is formed in the solution. Calcium chloride ($CaCl_2$-$2H_2O$, Sigma Aldrich) and sodium silicate ($Na_2Si_3O_7$, 27 wt% SiO_2, 1.39 g/mL, Sigma Aldrich) are added in sequence. After all the chemicals are added, the solution pH is adjusted to pH 8.2 using NaOH. In addition to the aluminum hydroxides, calcium silicate is formed, and at least potentially, SAS could form. Tests were also done with surrogates prepared following the same procedures, but without calcium chloride, to focus attention on the Al-based precipitates.

Settling rate tests were conducted for the CCI plant-specific surrogate using a 250-mL graduated cylinder. Figure 10 shows settling rate test results for these surrogates. The settling behavior observed in the bench top tests is slightly faster than those reported by CCI

for this chemistry, but the overall trend appears to be consistent with that in the CCI tests. A settling rate test was conducted with a higher Al concentration, 250 ppm, instead of the nominal 115 ppm. The settling rate for the 250 ppm Al surrogate was slightly less than that for the 115 ppm surrogate, but after 4 hours the total precipitate volume approached that of the 115 ppm surrogate. When sodium aluminate solution was added to borated water, the solution became cloudy but precipitate particles were not visible to the naked eye for at least several minutes. After 1-2 hours under stagnant condition, flocculation was observed. The precipitate formed by the addition of the sodium aluminate is aluminum hydroxide. Addition of calcium as calcium chloride did not make any significant change in solution, but the addition of sodium silicate solution resulted in the formation of large, visible precipitates (floccules) in the solution. The visible precipitates formed after the silicate addition appears to be calcium silicate. After 30 minutes most of big floccules settled, but the supernate solution was still cloudy, which suggests that aluminum hydroxide precipitates are very small compared to calcium silicate particle. During the settling rate tests, samples were taken from the supernates of the 115 and 250 ppm solutions after 30 minutes. The ICP analysis of the supernate samples is summarized in Table 1. The Al, B, and Ca concentrations in the filtered 115-ppm Al sample are comparable to those reported for a similar industry test. But the Si concentration is higher than the industry results. Unfiltered samples indicate the supernatants have aluminum hydroxide precipitates larger than 20 nm and some amount of calcium silicate. When the Al concentration is increased, the Al concentration in the supernate increased, as expected, but a decrease in Ca and Si concentration was observed. A higher Al concentration may enhance the calcium silicate precipitation. The enhancement of flocculation by high ionic strength will be discussed in a later section.

Table 1. Supernate chemical compositions and particle size distributions of ANL CCI surrogate samples compared to industry's test result.

Solution Identification		Supernate Concentration, ppm					Particle Size, μm		
		Al	B	Ca	Si	Na	<5%	<50%	<90%
ANL	115 ppm Al CCI plant-specific (0.02 μm filtered)	6.88	2450	35.6	234	784	9.2	18.7	36.4
	115 ppm Al CCI plant-specific (unfiltered)	11.2	2380	39.7	246	806			
	250 ppm Al CCI plant-specific (0.02 μm filtered)	21.2	2370	20.0	221	814	7.6	18.2	38.6
	250 ppm Al CCI plant-specific (unfiltered)	38.6	2400	25.5	231	819			
115 ppm Al CCI plant-specific		6.8	2600	45	110[a]	NA[b]	12	22	38

[a] concentration as SiO_2

[b] data are not available

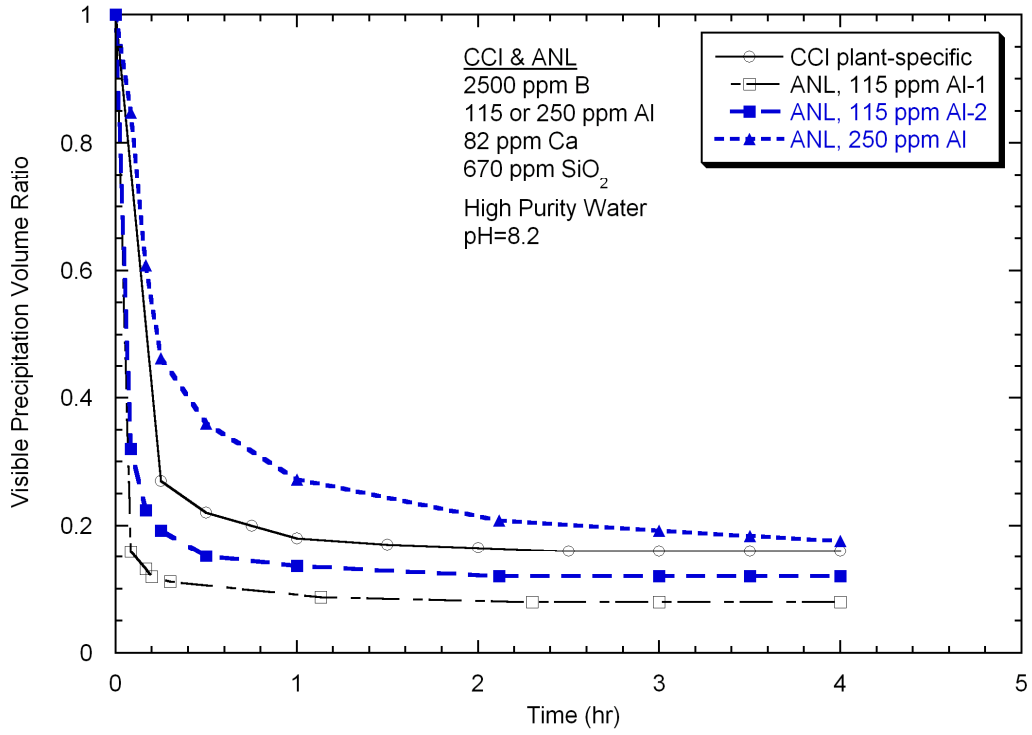

Figure 10. Visible precipitation volume ratio time history in the CCI-type surrogate solution compared to the CCI surrogate test result.

Figure 11 shows the particle size distributions of CCI plant-specific precipitates. Figure 11a indicates the sensitivity of the size distribution to ultrasonic deflocculation. The particles, mainly calcium silicate, seem to be easily flocculated, but also easily deflocculated by external force. As mentioned earlier, sump flow velocities are low so that particle size before the ultrasonic deflocculation may be more representative of those to be expected. Figure 11b shows particle size distributions as a function of total Al concentration. There is not a significant difference in terms of particle size even though there is a difference in total settled precipitation volume. The particle size distribution is consistent with industry results as shown in Table 1. The median particle size of this surrogate is 18-19 μm, which is slightly larger than that of the WCAP AlOOH surrogate with 2.2 g/L mixing concentration, but the settling rate is much higher than for the WCAP surrogate. The hydration of the particles which affects the density may be different. The CCI-type surrogate also has a much lower particle number density, which decreases the effective drag on the particles. The relationship between the settling rate and particle size and degree of hydration is discussed later.

Surrogates produced using the CCI approach, but without calcium chloride additions, were also examined. Various concentration of Al solution as sodium aluminate were added to high purity water containing 2500 ppm B, and then 670 ppm SiO_2 as sodium silicate was added. The final solution pH was adjusted to 8.2 using NaOH. Figure 12 shows the variation of solution turbidity as a function of total Al concentration in borated water after 2 hours. Initially, the 115 ppm Al solution was cloudy, but over 2 hours the solution became almost clear. The 250 and 500 ppm Al solutions also became clearer, but not as clear as the 115 ppm Al solution. The 1000 ppm Al solution was cloudier than 500 ppm Al solution. Solutions with concentrations equal to or less than 500 ppm Al showed no sedimentation for times up to 11 days. The 1000 ppm Al solution did not show any sedimentation for 7 days. Based on the settling behavior, it was expected that the particle size of these surrogates would be much smaller than previous surrogates. To analyze nanometer-range particles, a different type of particle analyzer (Zeta Potential Analyzer, Brookhaven Instruments Corporation) was used. The particle size distributions for the Al surrogates in borated solution are shown in Figure 13. (The results for the 1000 ppm Al solution were determined by laser diffractometry.) The median particle size tends to increase as the total Al concentration increases, but the particle sizes are around 100 times smaller than the WCAP AlOOH or SAS surrogates. Detailed results of the particle analysis of these solutions are given in Appendix B.

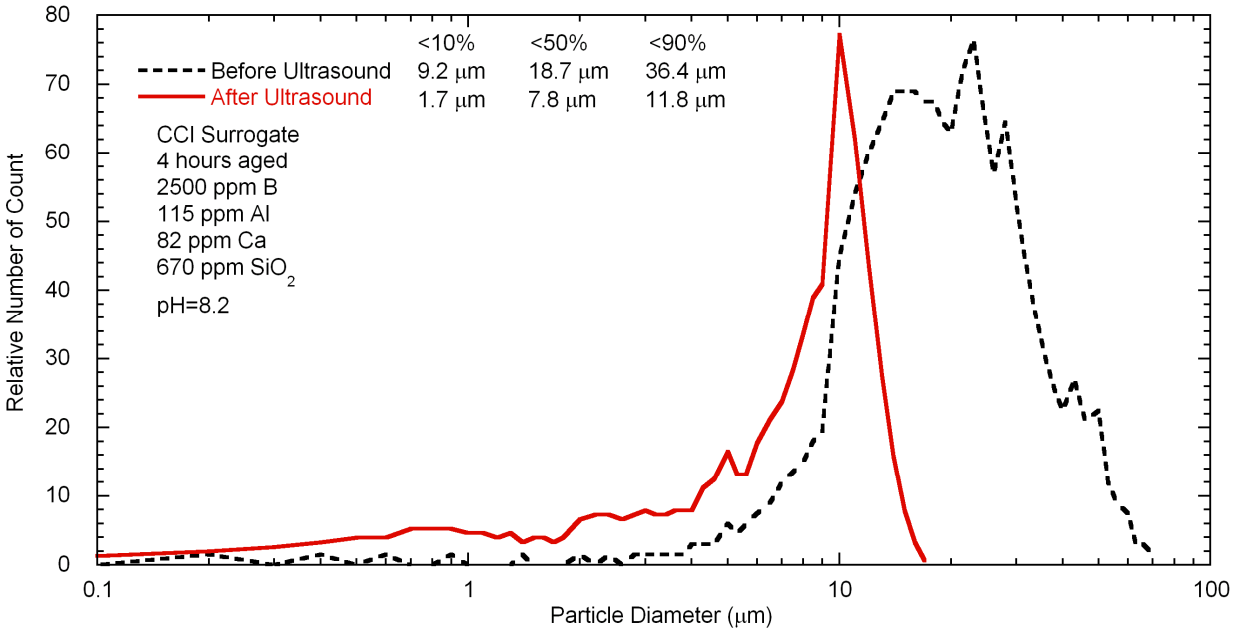

(a) Effect of ultrasonic deflocculation

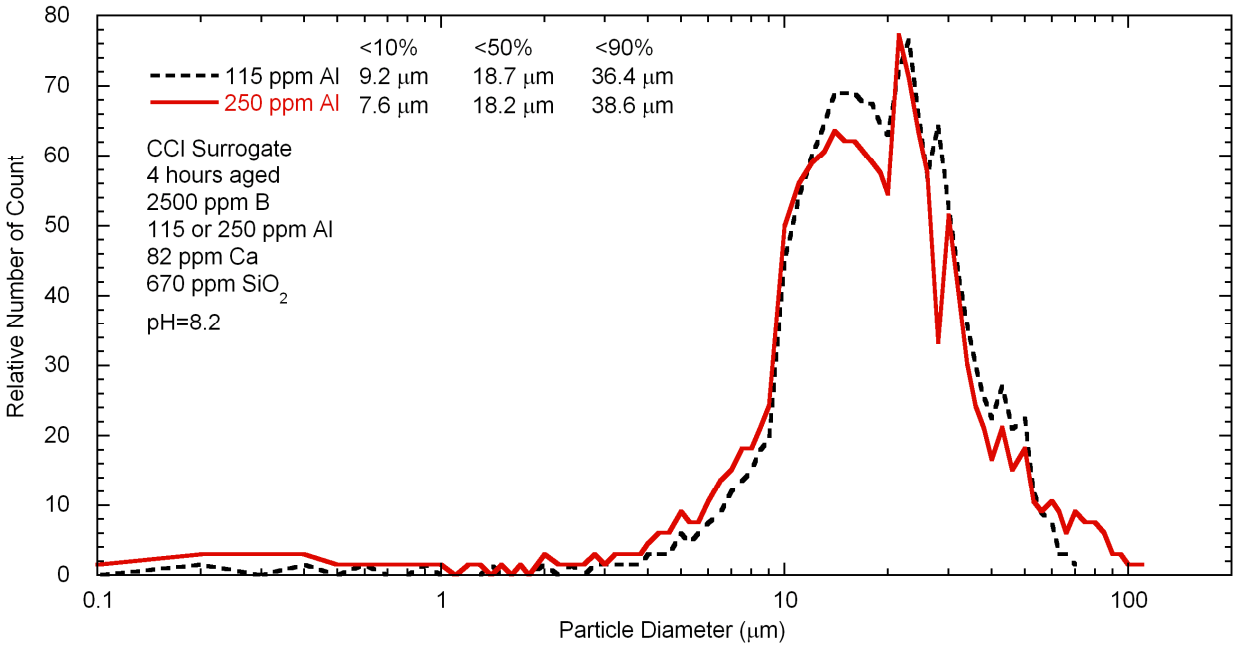

(b) Effect of aluminum concentration

Figure 11. Particle size distributions of CCI surrogates including Ca as function of (a) ultrasonic deflocculation and (b) aluminum concentration.

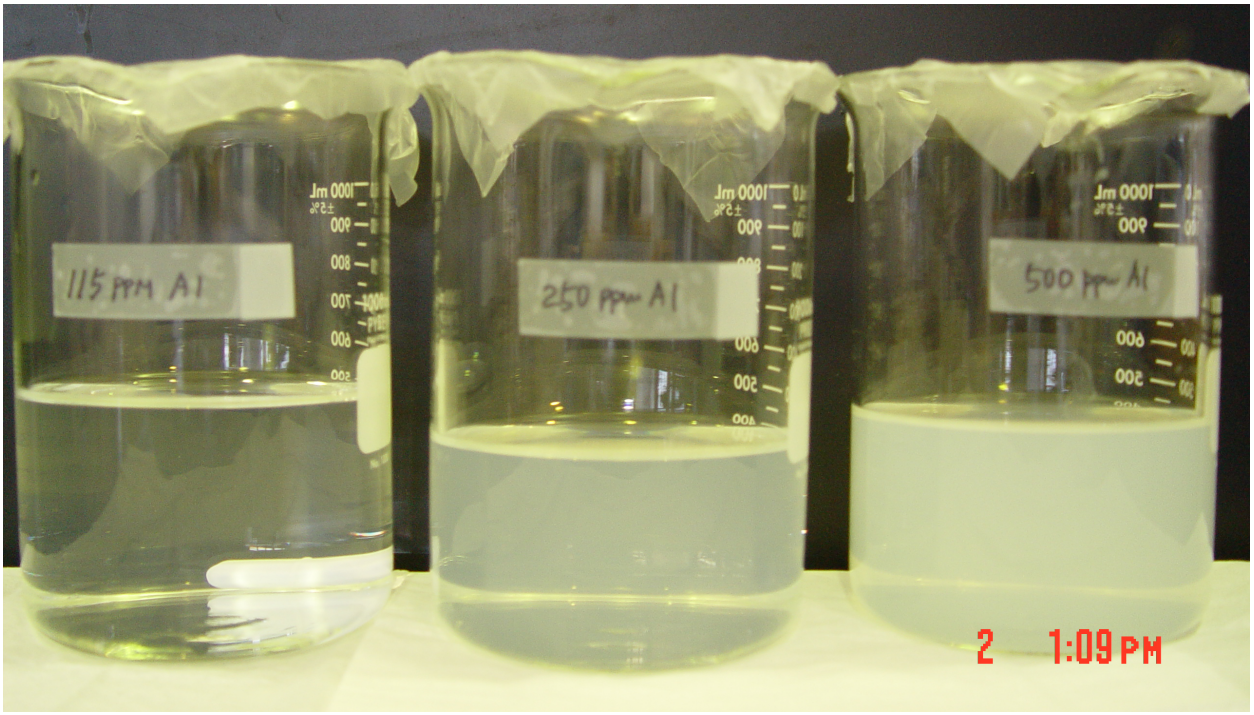

Figure 12. Solution turbidity variation as a function of total Al concentration in borated water after 2 hours (Left: 115 ppm Al, middle: 250 ppm Al, and right: 500 ppm Al).

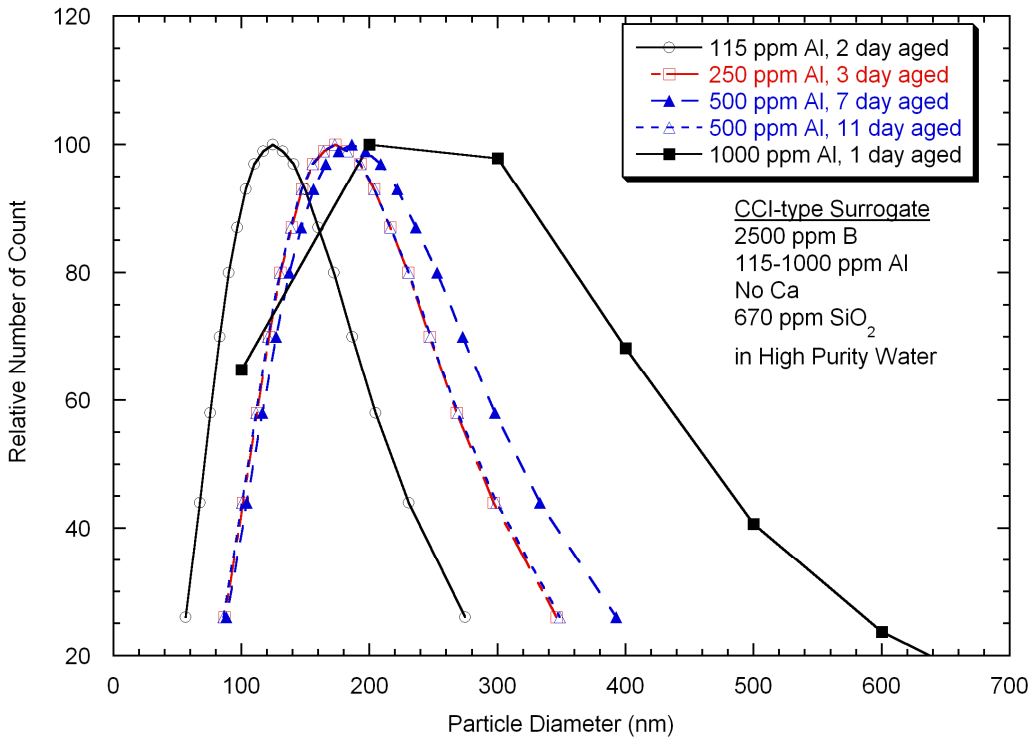

Figure 13. Particle size distributions of CCI-type surrogates in borated water without Ca as a function of Al concentration in surrogate solution.

Loop Head Loss Test – CCI Type Precipitates

A head loss test was conducted using the aluminum hydroxide surrogates made by the CCI procedure described in the bench top test results. In an attempt to closely control the amounts of aluminum precipitates in the loop, this first loop test deviated from the CCI method of direct chemical addition. Instead, precipitates were formed by mixing solutions with concentrations corresponding to those specified in the CCI procedure outside of the test loop, and then controlled amounts of surrogate product were added to the vertical head loss loop.

The loop was filled with high purity water and the loop water temperature raised to 120 F to help dissolution of boric acid powder. When the water pH became stable, the loop water temperature was decreased to 80°F and 670 ppm SiO_2 as sodium silicate solution was added. The final loop water pH was adjusted to 8.2 using NaOH.

Figure 14 shows the pressure drop, screen approach velocity and loop water temperature time history. As noted in Figure 14, addition of 2.0 ppm Al equivalent of the 115 ppm Al concentration surrogate produced no increase in pressure drop. Addition of 4.2 ppm Al equivalent of the 250 ppm Al surrogate also did not produce any significant change in pressure drop. The fine Al surrogates are either ineffective in producing head loss or dissolve very quickly in the loop water. Additions of 8.5 ppm and 16.9 ppm Al equivalent of the 500 ppm Al and 1000 ppm Al surrogates, respectively, resulted in an immediate small increase of 0.05-psi, but the pressure drop readily came back close to the initial point. However, following the addition of the 1000 ppm Al surrogate there was gradual increase of the pressure drop. Since the loop water temperature was controlled at constant value of 80°F overnight as shown in Figure 14b, the increase in pressure drop does seem due to the surrogate addition rather than a loop water temperature change. The total accumulated Al concentration in the loop was 32 ppm. The results seem to indicate that particles less than 0.5 μm in size do not get trapped in the NUKON bed and are not effective in producing head loss. After the 32 ppm Al equivalent addition, an additional 2 ppm Al equivalent of 115 ppm Al surrogate including Ca was added, which resulted in an immediate head loss of 0.25 psi, but the pressure drop quickly decreased presumably because the calcium silicate precipitates dissolved in the loop water solution, which did not have any Ca. The differences in head loss associated with surrogates with and without Ca can be explained in terms of the particle size differences shown in Figures 11 and 13.

Industry head loss tests generally have used tap water rather than high purity water. In the CCI test approach, the chemicals are introduced directly into the borated water test loop rather than being used to prepare a precipitate solution that is then added to the loop as in the WCAP procedure and as was done in the first loop test with these surrogates. Hence, to more accurately simulate the CCI-type test, a head loss test was conducted with tap water instead of high purity water and with direct introduction of the chemicals into the vertical head loss test loop. The major dissolved impurities in ANL tap water are 32 ppm Ca, 11 ppm Mg, 1 ppm Si, and 7 ppm Na, as shown in Table A2. Anions like chloride and sulfate are probably present, but anions were not analyzed. The Al concentration in the tap water is below the detection limit, 0.5 ppm. The chemical addition procedure followed that used by CCI when conducting head loss tests. The sequence of additions follows that used in the bench tests: sodium aluminate, calcium chloride, and sodium silicate, but initially only 40% of the total chemical contents are added. In the industry tests, the rest of the chemicals are added in batches to get 60, 80, 100 up to 140%. Since Ca concentration in ANL tap water is quite close to 40 % of the final concentration of 82 ppm Ca, no Ca was to be introduced in the first batch. This mimics the test approach used by CCI when Ca is present in significant amounts in the tap water.

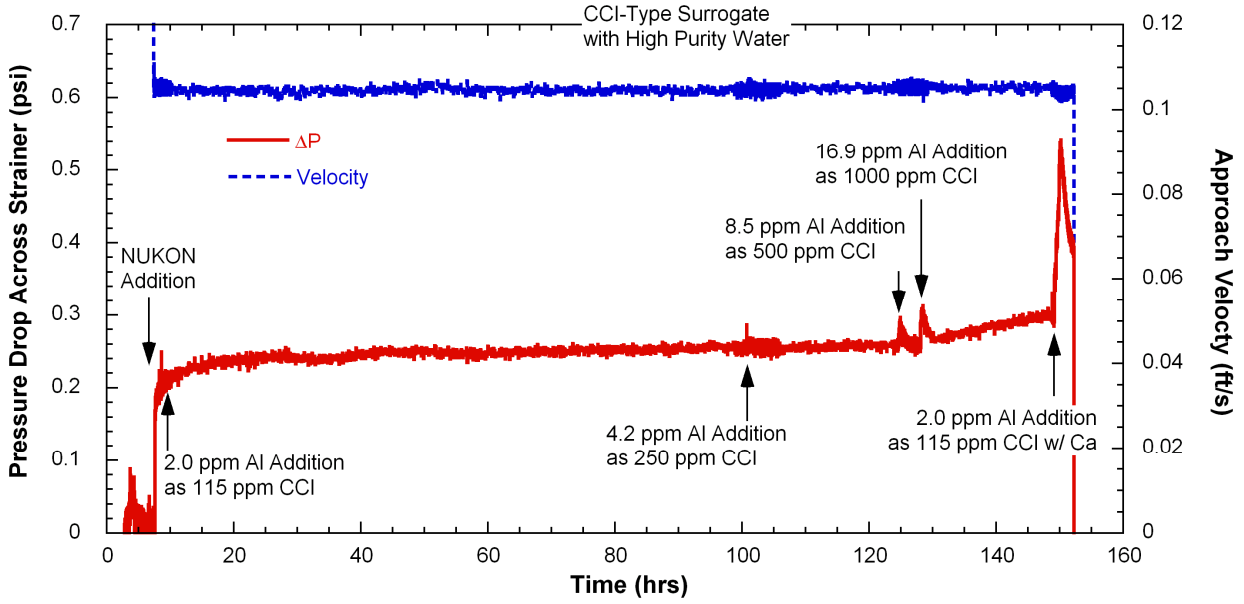

(a)

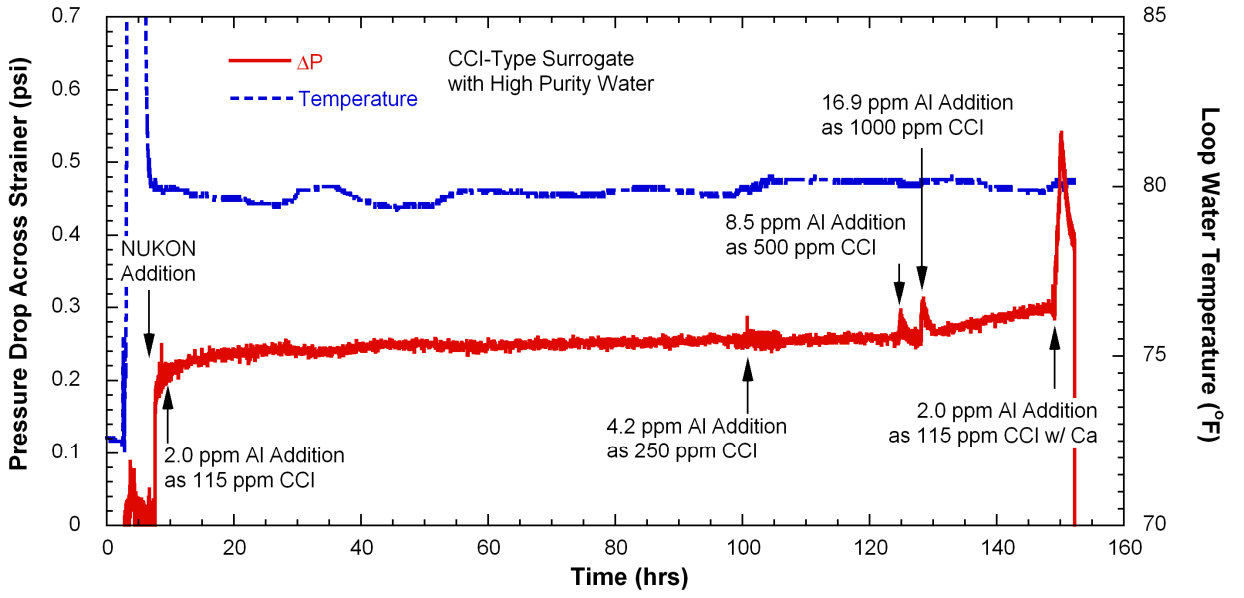

(b)

Figure 14. Pressure drop and (a) screen approach velocity or (b) loop water temperature time history in loop test using the CCI -type chemicals to prepare precipitate solutions with and without Ca.

Figure 15 shows the pressure drop and screen approach velocity time history in the loop test. As shown in Figure 15a, as soon as 5.7 ppm Al as sodium aluminate solution with a concentration of 7000 ppm Al was added, the pressure drop started to increase and kept increasing over 2 hours. When the head loss reached a loop capacity limit, the pump was shut down and turned on again after one hour and the test was continued for three days. As shown in Figure 15b, the pressure drop had stabilized at a slightly lower value than before. The large pressure drop seems to suggest that the precipitates formed in this loop test are much larger and more stable than the very fine Al hydroxide formed in the bench top tests that use high purity water and silicate solution. Consistent with our bench top test, this loop test result suggests that aluminum hydroxide precipitates are very stable in tap water even if the total Al concentration is only 5.7 ppm (112.4 g/m^2 AlOOH). ICP analyses for the loop water samples showed no detectable dissolved Al over the test period, as shown in Table A2.

The aluminum hydroxide precipitation formed in borated high purity water with silicate appears to be relatively easily dissolved and in any case the particle sizes are so small that they do not cause significant head loss, at least with the glass fiber bed used in our tests. In contrast, the aluminum hydroxide precipitate formed in borated tap water without silicate is not dissolved and has much larger particle sizes. Possible reasons for this difference between precipitates in high purity and tap water are discussed in a later section.

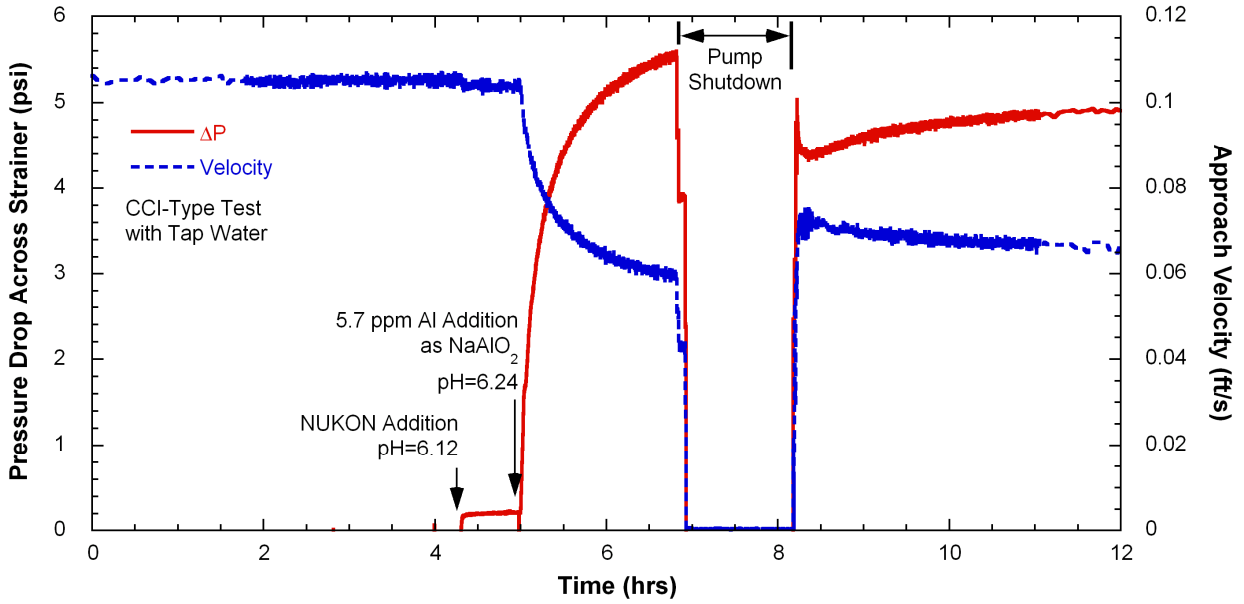

(a) First 12 hours

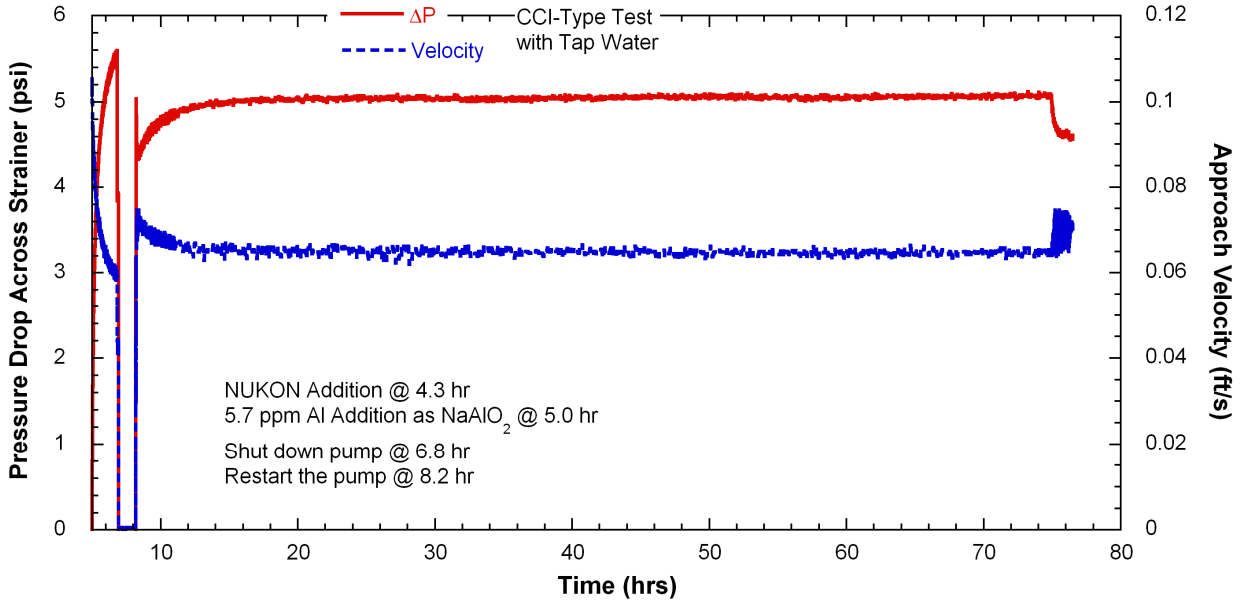

(b) Full time history

Figure 15. Pressure drop and screen approach velocity time history in loop test following the CCI's test procedure with tap water for (a) the first 12 hours and (b) full time range.

Discussion

Particle Size Effect on Settling Velocity

Assuming that the particles of interest are spherical in shape and fall in a viscous medium, a force balance equation is given as Eq. (1):[5]

$$\underset{\text{(Gravity force)}}{\frac{3}{4}\pi R^3 \rho_s g} = \underset{\text{(Buoyancy force)}}{\frac{3}{4}\pi R^3 \rho_l g} + \underset{\text{(Drag force)}}{6\pi\mu R v}, \quad (1)$$

where R is the radius of the particle, ρ_s and ρ_l are the densities of the solid sphere and the fluid, μ is the viscosity of the medium, g is the acceleration due to gravity, and v is the settling velocity in the medium. Solving this equation for the velocity gives Stokes Law:

$$v = \frac{1}{18} D^2 (\rho_s - \rho_l) \frac{g}{\mu}, \quad (2)$$

where D is the diameter of the particles.

Figure 16 shows the measured settling velocities of the WCAP AlOOH and SAS surrogates for the first one hour compared to the velocities predicted by Eq. (2) for a range of diameters. The measured settling velocity for the first one hour was estimated by linearly fitting data shown in Figures 1 and 5. The "particle diameter" in Figure 16 is the median diameter of each surrogate. The solid line assumes that the precipitates are 92% water, consistent with measurements at LANL[6], and that the viscosity of the fluid in which the particle is falling is the same as pure water at room temperature so that a particle flows through the pure water without any other restriction. The calculated settling velocities are larger than the measured velocities. The dashed line obtained by varying the value of the viscosity until the calculated settling velocity matched the measured velocity reasonably well. This resulted in a value for the viscosity that is 3 times higher than pure water. This is an "effective" viscosity that probably reflects the effects of departures from the infinite dilution model with no particle interactions and actual changes in the viscosity of the WCAP surrogate solution due to the relatively high concentration of particles and dissolved ions. The differences could also reflect uncertainty in the actual degree of hydration. As particle sizes become bigger and concentrations increase, the deviation of measured values from the theoretical line becomes larger. This is consistent with an even higher particle-to-particle interaction at higher total concentration. An estimate of settling velocity considering the colloidal characteristics of the surrogates is discussed in a later section.

Al Hydroxide Precipitation in Borated Water

As demonstrated in the loop tests, the characteristics of the aluminum hydroxide precipitates in borated water and their effectiveness in producing head loss seem to strongly depend on whether the solution is made from high purity water or tap water. To better understand this behavior, several bench top tests were conducted with tap water. Sodium aluminate solution having 7000 ppm Al was added to borated tap water without stirring to make a solution with 115 ppm Al. As soon as the sodium aluminate solution was added, a heavily flocculated precipitate was formed and quickly settled in a stagnant solution. Figure 17 shows the particle size distributions of the aluminum hydroxide precipitation. The precipitates

were easily breakable as shown by the results after ultrasonic deflocculation in Figure 17. The bench top test results suggest the reason that precipitates formed in borated tap water are more effective in producing head less is the large particle size compared to those of precipitates formed in borated high purity water. A study by Csempesz and Rohrsetzer[7] showed that higher ionic strength due to dissolved salts can induce flocculation in a suspension that does not flocculate in a low ionic strength solution. Tap water has much higher levels of dissolved cations and anions than high purity water. This higher ionic strength may enhance the flocculation of aluminum hydroxide precipitates, which increases the effectiveness of the precipitates in producing head loss.

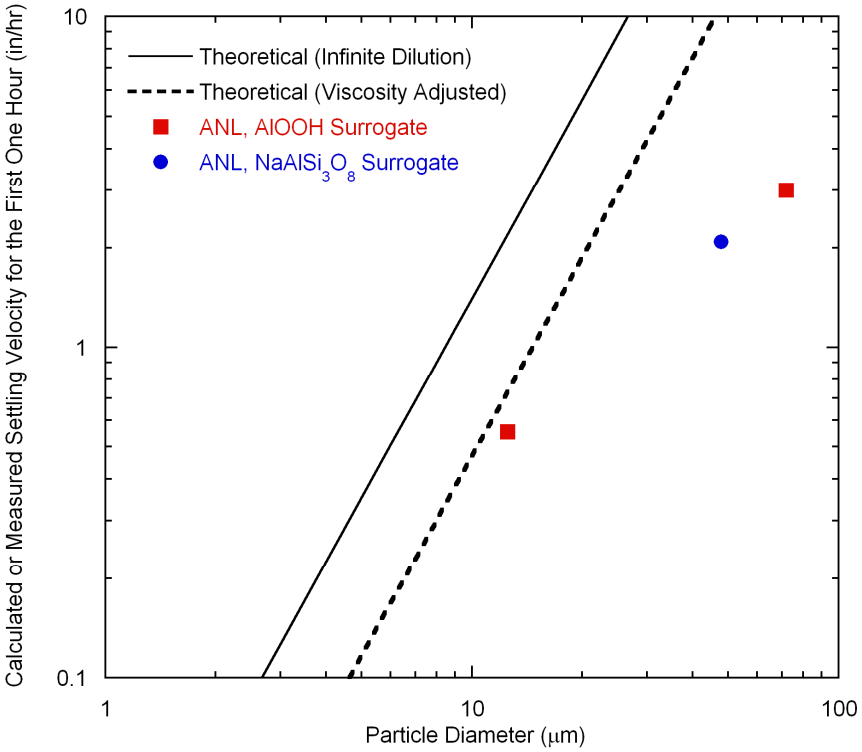

Figure 16.
Measured settling velocities of AlOOH and sodium aluminum silicate surrogates for the first one hour compared to predicted velocity using Stokes' Law.

Additional bench top tests were also conducted with borated high purity water. Sodium aluminate was added without stirring to borated high purity water to create a 115 ppm Al solution. The solution became cloudy but immediate flocculation did not occur as was observed in borated tap water. After about 1 hour, visible cotton-ball like precipitates were observed to have formed, but they did not readily settle. Left overnight the solution did not become clear. Then 313 ppm Si (=670 ppm SiO_2) as sodium silicate solution was added to the solution. As soon as sodium silicate solution was added, the solution became clearer. After 4 hours the solution was still slightly cloudy, but the turbidity decreased drastically. To determine whether the apparent increase in solubility was due to the silicate itself or the associated change in pH, another 115 ppm Al solution in borated high purity water was made and the pH adjusted with NaOH to get a pH of 8.2, which matched that of the solution with sodium silicate, without adding sodium silicate. The pH-adjusted 115 ppm Al solution showed a slight change in of turbidity, but the effect was much less than observed in the solution to which sodium silicate was added. A study by Boisvert and Jolicoeur[2] showed that the silicate specifically inhibits Al_{13} [polyoxocation $AlO_4Al_{12}(OH)_{24}$-12H2O (7+)] formation and promotes

formation of unidentified soluble aluminosilicate species. Adu-Wusu and Wilcox[3] studied the reaction of silicate with gibbsite (i.e., stable crystalline $Al(OH)_3$) in sodium aluminate solution. The study showed that the adsorption of silicate on gibbsite seed crystals reduces the gibbsite crystallization and increases the equilibrium solubility of gibbsite. These studies seem to support the findings in our bench top and loop head loss tests that suggest that sodium silicate promotes the dissolution of aluminum hydroxide precipitates in borated high purity water. Vender loop tests are typically conducted with tap water, not high purity water.

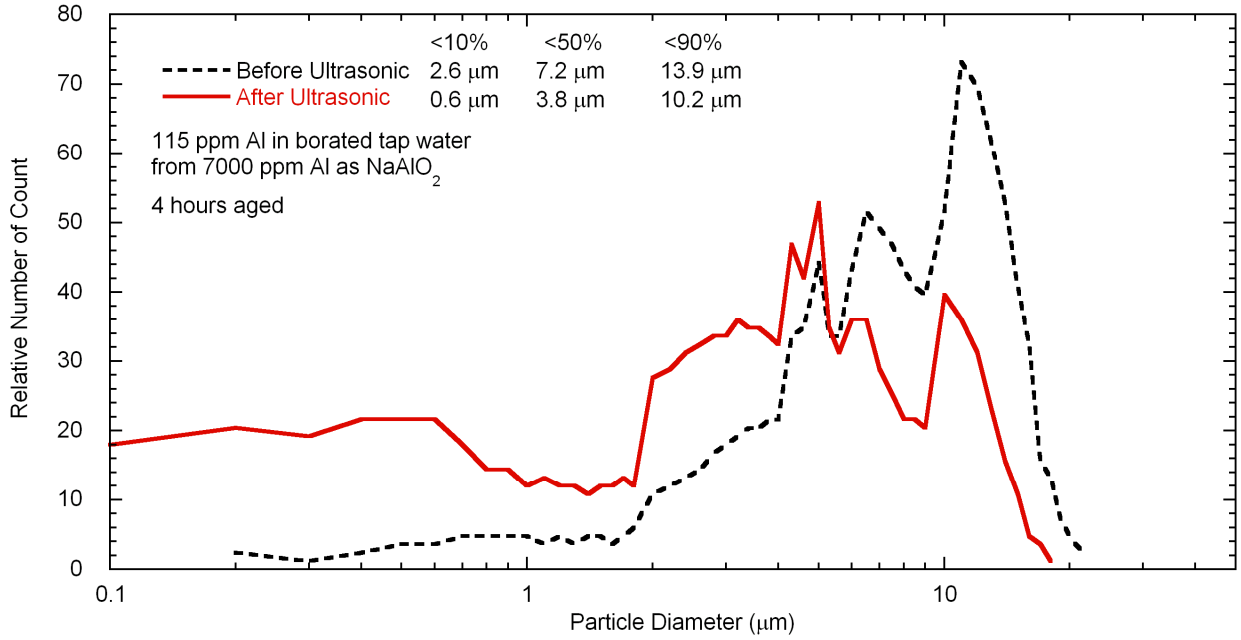

Figure 17. Particle size distributions of CCI plant-specific surrogate solution containing 115 ppm Al from 7000 ppm Al as sodium aluminate solution.

Colloid Aggregation

There are two distinct, limiting regimes of irreversible colloid aggregation.[8] Diffusion-limited colloid aggregation (DLCA) occurs when there is negligible repulsive force between the colloidal particles, so that the aggregation rate is limited solely by the time taken for clusters to encounter each other by diffusion. Reaction-limited colloid aggregation (RLCA) occurs when there is still a substantial, but not insurmountable, repulsive force between the particles, so that the aggregation rate is limited by the time taken for two clusters to overcome this repulsive barrier by thermal activation. Lin et al.[8] showed that each of these limiting regimes is universal, independent of the chemical details of the particular colloid system. Each regime has its own unique particle size distribution characteristic. Comparison of the distribution predicted for RLCA type colloids with the observed distributions suggests that all the surrogates described in this report are of the RLCA type, except for CCI-type solutions using high purity water. The particle size distributions for these solutions, which are shown in Figure 13, do not fit to that of RLCA. These small particles may be electrically neutralized by silicate and limited by DLCA.

Lin et al.[9] characterize the size of a colloidal cluster of mass M by its radius of gyration R_g and have

$$M = \left(\frac{R_g}{a} \right)^{d_f}, \tag{3}$$

where a is the radius of a constituent single particle and d_f is the fractal dimension of clusters. M represents the number of particles in the cluster. The fractal dimension d_f reflects properties of the radially averaged structure of the clusters. The cluster size distribution N(M) can be described as a power-law form with an exponential cutoff

$$N(M) = AM^{\tau} \exp\left(-M / M_c\right), \tag{4}$$

where A is constant, τ is the exponent for the cluster distribution, and M_c is the cutoff cluster mass. If Eq. (3) is introduced and M is replaced with the radius R_g, a cluster diameter distribution $N(D_g)$ can be described as a similar form:

$$N(D_g) = k D_g^{\tau d_f} \exp\left(-\left(\frac{D_g}{D_{g,c}} \right)^{d_f} \right), \tag{5}$$

where k is a constant, D_g is the diameter of gyration, and $D_{g,c}$ is the cutoff diameter. Lin et al.[9] showed experimentally that the fractal dimensions of different chemical clusters limited by RLCA are all d_f=2.1±0.05. The exponent for the power-law cluster distribution, τ is 1.5±0.1.[9] Using measured particle size distribution data for the WCAP surrogate, a cutoff diameter was derived by fitting Eq, (5) to the observed distributions using least-squares. Figure 18 shows that Eq. (5) provides a good representation of measured particle size distribution over the entire particle size range. Similar analyses show that the particle size distribution of all the surrogates described in this report, except for as noted previously, are well-described by Eq. (5), no matter what the total concentration or the chemical nature of the colloid system is. Table 2 gives a comparison of the fitted cutoff diameter, $D_{g,c}$, with the measured median particle diameter. The agreement is typically within 10%.

In Eq. (4) the cutoff mass M_c is dependent on time and grows exponentially, so that the cutoff diameter also grows exponentially.[9] Although we did not characterize the variation of particle size as a function of time, based on the potential growth of the particles with time, it is recommended that once surrogates are made, all surrogates should be used relatively quickly to avoid the particle growth and to assure reproducibility of results. Performance-based tests using settling times can be used to determine acceptance.

The settling velocity of colloidal clusters limited by RLCA can be described using the fractal dimension d_f of the clusters and the constituent particle size a in Eq. (3) [9];

$$v = \frac{2g}{9\mu}\left(\rho_a - \rho_o\right) a^2 \left[\frac{R_h}{a} \right]^{d_f - 1}, \tag{6}$$

where ρ_a is the density of the constituent particles, ρ_o is the density of water, and R_h is the hydrodynamic radius of the cluster, which can be assumed to be the same as R_g. Assuming the viscosity is same as pure water and the density of the constituent particles is that of aluminum hydroxide, theoretical settling velocities as a function of the constituent particle size a, which is smaller than the cluster size, are shown in Figure 19. The slopes in Figure 16,

based on Stokes' Law for an individual particle are steeper than the observed values, but the slopes predicted by Eq. (6) are in good agreement with measured values. Previous estimates of constituent particle size ranged from 15-30 nm,[6] which is not too far from the values needed to get good agreement with the observed data. It appears that AlOOH surrogate and SAS surrogate may have similar constituent particle sizes.

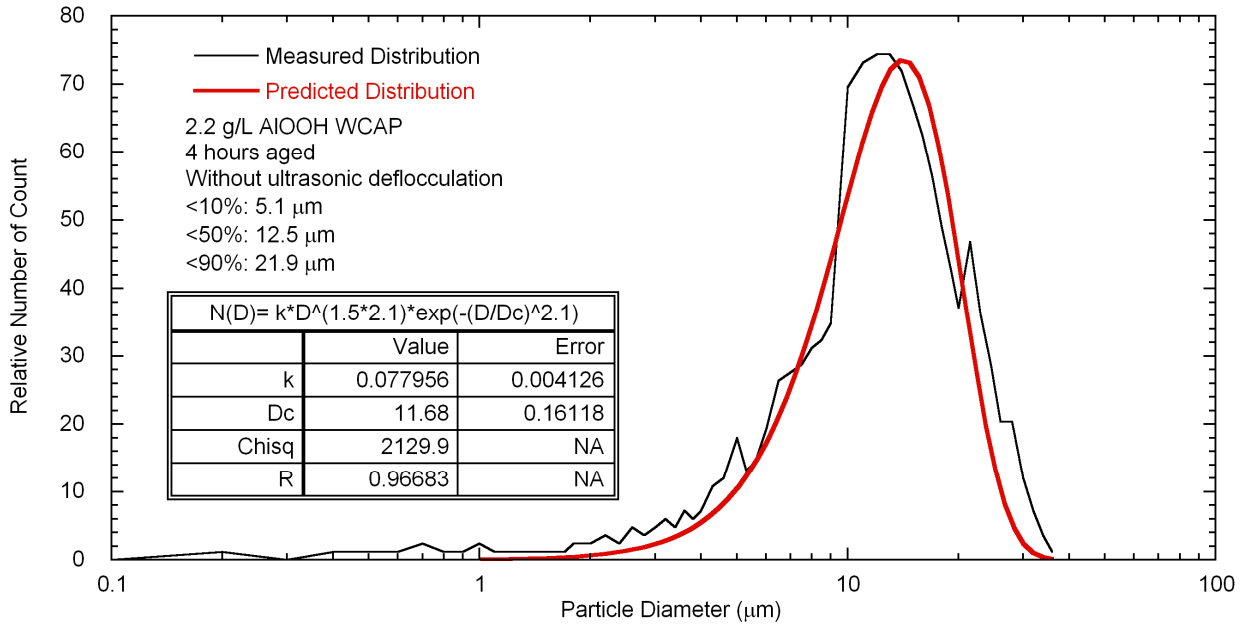

Figure 18. Fitted particle size distribution of the WCAP AlOOH surrogate using an analytical distribution equation compared to measured distribution.

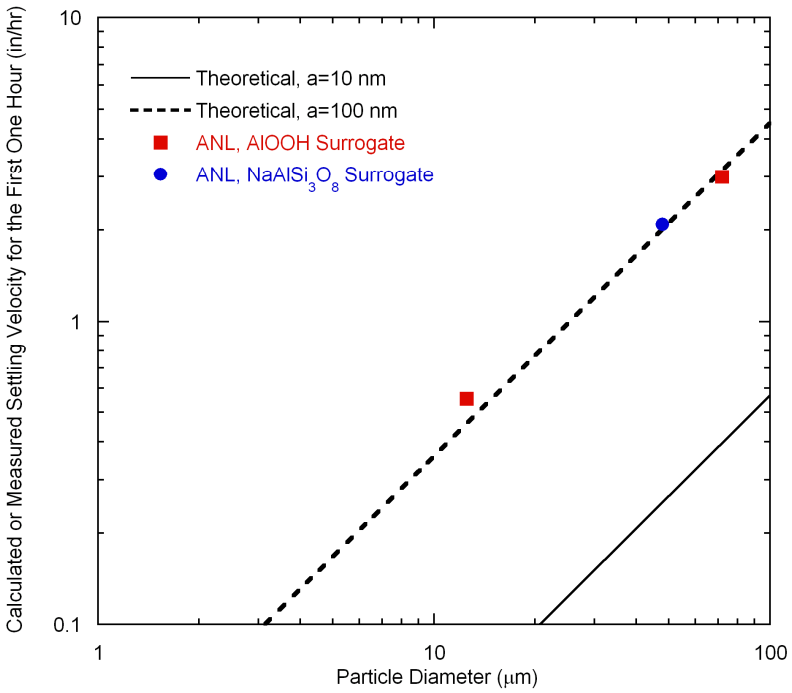

Figure 19.
Predicted settling velocity based on an analytical distribution equation for colloidal particle diameter compared to measured settling velocity for the WCAP surrogates.

Table 2. Measured median particle diameter and cutoff particle diameter derived from fitted results using Eq. (5).

Surrogate Type	Possible Precipitates	Measured Median Particle Diameter, μm	Fitted Cutoff Particle Diameter, μm
1000 ppm Al, WCAP AlOOH	Aluminum hydroxide	12.5	11.7
115 ppm Al in Borated Water from 7000 ppm Al solution	Aluminum hydroxide	7.2	8.5
1000 ppm Al, WCAP SAS	Sodium aluminum silicate	47.8	47.9
115 ppm Al, CCI-type Surrogate	Al hydroxide & Calcium silicate	18.7	17.3

SUMMARY

Bench Tests

- The particle diameter of the WCAP AlOOH surrogates ranges between 13 and 72 μm depending on total aluminum concentration.
- The particle size of the WCAP SAS surrogates is larger than that of the AlOOH surrogates with the same Al concentration.
- The WCAP SAS surrogate is less stable in high purity water than the AlOOH surrogate and tends to dissolve at low concentrations. It is more stable in tap water even at low concentrations.
- Al hydroxide precipitates are more easily flocculated in borated tap water than in borated high purity water. This difference may be attributable to the difference in ionic strength.
- Silicate appears to act as a deflocculant for aluminum hydroxide precipitates and increase their solubility in borated high purity water. As a result, extremely fine aluminum hydroxide precipitates ranging between 100-500 nm in diameter can be formed in solutions with silicate additions.
- The initial settling rates of various surrogates are strongly dependent on their particle sizes, and the measured rates are reasonably consistent with theoretically predicted results.
- The particle size distributions of various surrogates are universal, consistent with the predictions of colloid aggregation theory.

Loop Head Loss Tests

- 1.5 ppm Al (29.6 g/m^2 AlOOH) as the WCAP AlOOH surrogate and 2.0 ppm Al (172 g/m^2 SAS) as the WCAP SAS surrogate caused significant head losses in the glass fiber bed.

- Extremely fine Al hydroxide precipitates produced in borated high purity water with silicate did not cause significant head loss in a loop test even with up to 33 ppm Al equivalent surrogate additions. As noted only 1.5 ppm (29.6 g/m^2 AlOOH) as the WCAP AlOOH surrogate was sufficient to exceed the loop capacity.
- Surrogates made in borated tap water without silicate by the CCI approach caused significant head loss with the total 5.7 ppm Al concentration (112.4 g/m^2 AlOOH). The Al hydroxide precipitates seem to be easily flocculated in the borated tap water due to the relatively high ionic strength by dissolved ions in tap water.

Acknowledgement

The authors are grateful to Dr. Carol J. Mertz of ANL for her help in the determination of the size distribution of the extremely fine particles produced by some surrogate procedures. The authors would also like to thank Mr. John J. Picciolo of ANL for his help in the analysis of particle size distributions of various samples.

References

1. C. B. Bahn, K. E. Kasza, and W.J. Shack, *Technical Letter Report on Follow-on Studies in Chemical Effects Head-Loss Research; Studies on WCAP Surrogates and Sodium Tetraborate Solutions*, U.S. Nuclear Regulatory Commission, Washington, D.C., February 2007.
2. J.-P. Boisvert and C. Jolicoeur, "Influences of sulfate and/or silicate present in partially prehydrolyzed Al(III) flocculants on Al(III) speciation in diluted solutions," Colloids Surf. A: Physicochem. Eng. Aspects 155 (1999) 161-170.
3. K. Adu-Wusu and W.R. Wilcox, "Kinetics of Silicate Reaction with Gibbsite," J. Colloid Interface Sci. 143 (1991) 127-138.
4. A. E. Lane, T. S. Andreychek, W. A. Byers, R. J. Jacko, Edward J. Lahoda, and Richard D. Reid, *Evaluation of Post-Accident Chemical Effects in Containment Sump Fluids to Support GSI-191,* WCAP-16530-NP, Westinghouse Electric Company LLC, 2006.
5. K. K. Das and P. Somasundaran, "A Kinetic Investigation of the Flocculation of Alumina with Polyacrylic Acid," J. Colloid Interface Sci. 271 (2004) 102-109.
6. M. Klasky, J. Zhang, M. Ding, B. Letellier, D. Chen, and K. Howe, *Aluminum Chemistry in Prototypical Post-LOCA PWR Containment Environment,* NUREG/CR-6915, U.S. Nuclear Regulatory Commission, Washington D.C., 2006
7. F. Csempesz and S. Rohrsetzer, "The Effect of Polymer Bridging on the Flocculation Kinetics of Colloidal Dispersions," Colloids Surf. 31 (1988) 215-230.
8. M. Y. Lin, H. M. Lindsay, D. A. Weitz, R. C. Ball, R. Klein, and P. Meakin, "Universality in Colloid Aggregation," Nature 339 (1989) 360-362.
9. M. Y. Lin, H. M. Lindsay, D. A. Weitz, R. C. Ball, R. Klein, and P. Meakin, "Universal Reaction-limited Colloid Aggregation," Phys. Rev. A 41 (1990) 2005-2020.

Appendix A: Raw Data for ICP Analysis

Table A1. Summary of ICP analysis for the Westinghouse SAS surrogate dissolution bench top test samples.

Sample ID	Description	Nominal [Al], ppm	Measured Concentration, ppm					
			Al	Ca	Mg	K	Si	Na
SAS-02	Surrogate in high purity water, 0.45 μm filtered	1.5	0.77	<0.5	<0.5	<0.5	4.34	12.6
SAS-03	Surrogate in high purity water, 0.45 μm filtered	1.5	0.77	<0.5	<0.5	<0.5	4.37	12.6
SAS-04	Surrogate in ANL tap water, 0.45 μm filtered	1.5	0.53	30.2	10.4	1.33	4.27	22.5
SAS-05	Surrogate in ANL tap water, 0.45 μm filtered	1.5	<0.5	30.3	10.4	1.32	4.21	22.1
SAS-06	Surrogate in ANL tap water, unfiltered	1.5	1.29	33.7	11.1	1.26	5.40	22.4
SAS-07	High purity water used in this test	-	<0.5	<0.5	<0.5	<0.5	<0.5	<0.5
SAS-08	ANL tap water used in this test	-	<0.5	33.7	11.2	1.37	0.89	7.35
SAS-09	Surrogate in high purity water, 0.45 μm filtered	3.0	1.47	<0.5	<0.5	<0.5	8.23	29.2
SAS-10	Surrogate in high purity water, 0.45 μm filtered	3.0	1.48	<0.5	<0.5	<0.5	8.19	29.2
SAS-11	Surrogate in ANL tap water, 0.45 μm filtered	3.0	<0.5	31.5	10.6	1.53	6.27	37.6
SAS-12	Surrogate in ANL tap water, 0.45 μm filtered	3.0	<0.5	31.5	10.6	1.46	6.27	37.2
SAS-13	High purity water in a Pyrex beaker	-	<0.5	<0.5	<0.5	<0.5	<0.5	<0.5
SAS-14	pH=9.1 solution in a Pyrex beaker	-	<0.5	<0.5	<0.5	<0.5	<0.5	10.9
SAS-15	Same as SAS-14 but one day aged in the Pyrex beaker	-	<0.5	<0.5	<0.5	<0.5	<0.5	11.2

Table A2. ICP analysis for chemical compositions in loop water samples from the CCI-type surrogate loop head loss test with tap water.

Sample #	Identification	Measured Concentration, ppm					
		Al	B	Ca	Mg	Si	Na
4-01	Tap water in the loop before NUKON addition	<0.5	<0.5	32.0	10.6	1.16	6.80
4-04	After NUKON and 5.7 ppm Al addition, 0.02 μm filtered	<0.5	2300	30.8	10.4	1.43	13.2
4-05	After NUKON and 5.7 ppm Al addition, 0.02 μm filtered	<0.5	2310	30.4	10.4	1.43	13.0
4-06	After NUKON and 5.7 ppm Al addition, unfiltered	<0.5	2300	31.3	10.5	1.44	13.3

Appendix B: Raw Data for Particle Analysis Using Zeta Potential Analyzer

115 ppm (Combined)

Effective Diameter: 124.4 nm
Polydispersity: 0.260
Avg. Count Rate: 20.6 kcps
Baseline Index: 4.5
Elapsed Time: 00:01:00

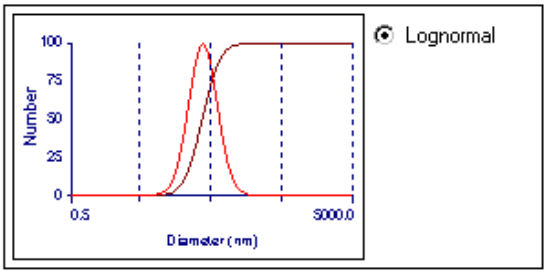

Run	Eff. Diam. (nm)	Half Width (nm)	Polydispersity	Baseline Index
1	12816.0	9473.2	0.546	0.0
2	148.1	80.5	0.296	0.0
3	133.9	71.7	0.286	0.0
4	134.7	73.0	0.294	0.0
5	124.4	63.5	0.260	4.5
6	127.1	64.8	0.259	0.0
7	129.1	66.5	0.265	0.0
8	130.9	67.5	0.266	0.0
9	129.8	64.5	0.247	0.0
10	129.3	64.4	0.248	0.0
Mean				
Std. Error				
Combined	124.4	63.5	0.260	4.5

Sample ID	115 ppm	(Combined)
Operator ID	nmk	
Elapsed Time	00:01:00	
Median Diam.	124.4 nm	
Mean Diam.	139.7 nm	
Polydispersity	0.260	
GSD	1.618	

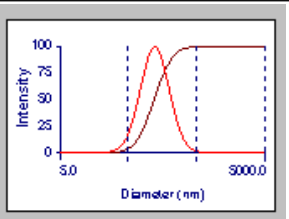

d(nm)	G(d)	C(d)	d(nm)	G(d)	C(d)	d(nm)	G(d)	C(d)
56.4	26	5	110.1	97	40	172.0	80	75
67.2	44	10	117.1	99	45	186.5	70	80
75.6	58	15	124.4	100	50	204.7	58	85
83.0	70	20	132.2	99	55	230.5	44	90
90.0	80	25	140.5	97	60	274.4	26	95
96.7	87	30	149.7	93	65			
103.4	93	35	160.1	87	70			

Intensity

Copy for Spreadsheet

Sample ID	115 ppm	(Combined)
Operator ID	nmk	
Elapsed Time	00:01:00	
Mean Diam.	169.6 nm	
Rel. Var.	0.222	
Skew	-0.507	

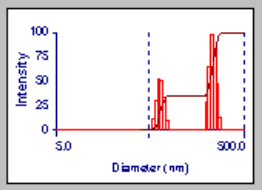

d(nm)	G(d)	C(d)	d(nm)	G(d)	C(d)	d(nm)	G(d)	C(d)
41.7	0	0	84.7	0	35	172.2	0	35
44.5	0	0	90.4	0	35	183.7	0	35
47.4	0	0	96.4	0	35	195.9	29	41
50.6	0	0	102.8	0	35	208.9	66	53
54.0	11	2	109.7	0	35	222.9	100	73
57.6	30	8	117.0	0	35	237.7	85	89
61.4	53	18	124.8	0	35	253.5	47	98
65.5	51	27	133.1	0	35	270.4	12	100
69.8	33	34	141.9	0	35	288.4	0	100
74.5	9	35	151.4	0	35	307.6	0	100
79.5	0	35	161.5	0	35	328.1	0	100

Intensity

250 ppm (Combined)

Effective Diameter: 173.3 nm
Polydispersity: 0.193
Avg. Count Rate: 445.7 kcps
Baseline Index: 9.2
Elapsed Time: 00:10:00

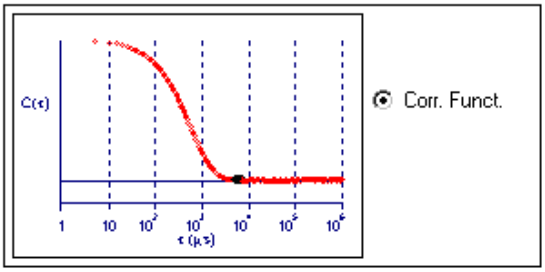

Run	Eff. Diam. (nm)	Half Width (nm)	Polydispersity	Baseline Index
1	180.0	80.1	0.198	9.9
2	175.8	73.2	0.174	4.7
3	177.4	78.9	0.198	8.5
4	177.6	80.4	0.205	9.9
5	171.0	82.5	0.233	7.7
6	171.8	74.7	0.189	8.5
7	170.4	79.0	0.215	9.7
8	168.4	68.9	0.168	6.8
9	170.5	70.2	0.170	7.5
10	167.9	70.3	0.175	6.1
Mean	173.1	75.8	0.192	7.9
Std. Error	1.4	1.6	0.007	0.5
Combined	173.3	76.2	0.193	9.2

Sample ID	250 ppm	(Combined)
Operator ID	cjm	
Elapsed Time	00:10:00	
Median Diam.	173.3 nm	
Mean Diam.	189.3 nm	
Polydispersity	0.193	
GSD	1.522	

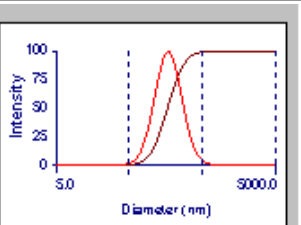

d(nm)	G(d)	C(d)	d(nm)	G(d)	C(d)	d(nm)	G(d)	C(d)
86.8	26	5	155.8	97	40	230.0	80	75
101.1	44	10	164.3	99	45	246.8	70	80
112.1	58	15	173.3	100	50	267.8	58	85
121.6	70	20	182.7	99	55	297.0	44	90
130.5	80	25	192.7	97	60	345.9	26	95
139.0	87	30	203.7	93	65			
147.4	93	35	216.0	87	70			

Intensity

Copy for Spreadsheet

Sample ID	250 ppm	(Combined)
Operator ID	cjm	
Elapsed Time	00:10:00	
Mean Diam.	209.7 nm	
Rel. Var.	0.122	
Skew	-1.092	

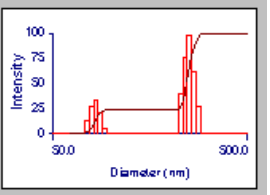

d(nm)	G(d)	C(d)	d(nm)	G(d)	C(d)	d(nm)	G(d)	C(d)
64.2	0	0	114.4	0	24	204.0	0	24
67.7	0	0	120.6	0	24	215.0	0	24
71.3	0	0	127.1	0	24	226.6	39	34
75.2	13	3	134.0	0	24	238.8	76	53
79.2	27	10	141.2	0	24	251.7	100	78
83.5	33	18	148.8	0	24	265.3	62	94
88.0	20	23	156.9	0	24	279.6	26	100
92.8	4	24	165.3	0	24	294.7	0	100
97.8	0	24	174.3	0	24	310.6	0	100
103.0	0	24	183.7	0	24	327.4	0	100
108.6	0	24	193.6	0	24	345.0	0	100

Intensity

500 ppm Al (Combined)

Effective Diameter: 173.0 nm
Polydispersity: 0.199
Avg. Count Rate: 446.9 kcps
Baseline Index: 9.2
Elapsed Time: 00:10:00

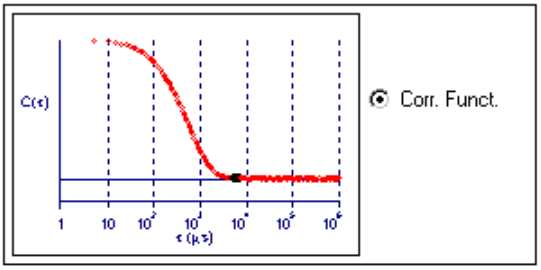

Run	Eff. Diam. (nm)	Half Width (nm)	Polydispersity	Baseline Index
1	184.4	78.7	0.182	7.8
2	176.5	80.8	0.210	7.9
3	178.7	82.4	0.213	9.9
4	169.1	70.7	0.175	8.9
5	171.8	79.4	0.214	7.4
6	168.0	76.7	0.208	7.6
7	171.8	76.9	0.200	9.9
8	170.6	74.9	0.193	8.6
9	167.8	75.4	0.202	7.0
10	166.4	74.3	0.199	7.7
Mean	172.5	77.0	0.199	8.3
Std. Error	1.8	1.1	0.004	0.3
Combined	173.0	77.2	0.199	9.2

Sample ID	500 ppm Al	(Combined)
Operator ID	cjm	
Elapsed Time	00:10:00	
Median Diam.	173.0 nm	
Mean Diam.	189.5 nm	
Polydispersity	0.199	
GSD	1.531	

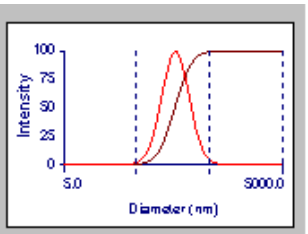

d(nm)	G(d)	C(d)	d(nm)	G(d)	C(d)	d(nm)	G(d)	C(d)
85.8	26	5	155.4	97	40	230.6	80	75
100.2	44	10	164.0	99	45	247.7	70	80
111.3	58	15	173.0	100	50	269.1	58	85
120.9	70	20	182.6	99	55	298.8	44	90
129.8	80	25	192.7	97	60	348.8	26	95
138.4	87	30	203.9	93	65			
146.9	93	35	216.3	87	70			

Intensity

Copy for Spreadsheet

Sample ID	500 ppm Al	(Combined)
Operator ID	cjm	
Elapsed Time	00:10:00	
Mean Diam.	215.2 nm	
Rel. Var.	0.162	
Skew	-0.568	

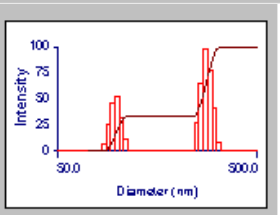

d(nm)	G(d)	C(d)	d(nm)	G(d)	C(d)	d(nm)	G(d)	C(d)
73.4	0	0	128.3	0	35	224.0	0	35
77.3	0	0	134.9	0	35	235.6	0	35
81.3	0	0	141.9	0	35	247.8	27	40
85.5	5	1	149.3	0	35	260.7	65	54
90.0	25	6	157.1	0	35	274.3	100	74
94.6	45	15	165.2	0	35	288.5	79	90
99.5	52	26	173.8	0	35	303.5	41	99
104.7	32	32	182.9	0	35	319.3	7	100
110.2	11	35	192.4	0	35	335.9	0	100
115.9	0	35	202.4	0	35	353.4	0	100
121.9	0	35	212.9	0	35	371.7	0	100

Intensity

500 ppm Al (Combined)

Effective Diameter: 186.2 nm
Polydispersity: 0.228
Avg. Count Rate: 447.5 kcps
Baseline Index: 9.2
Elapsed Time: 00:09:00

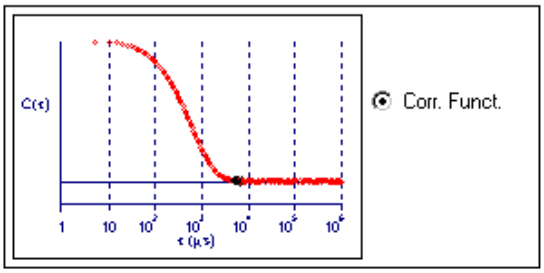

Run	Eff. Diam. (nm)	Half Width (nm)	Polydispersity	Baseline Index
1	207.0	96.9	0.219	3.3
2	200.5	93.4	0.217	8.4
3	189.2	93.0	0.242	6.2
4	192.4	90.0	0.219	9.4
5	183.4	89.9	0.240	7.6
6	182.4	87.9	0.232	9.5
7	179.7	84.9	0.223	9.9
8	183.3	89.7	0.240	6.0
9	180.7	82.8	0.210	9.6
10	180.9	88.6	0.240	8.8
Mean	185.8	88.9	0.229	8.4
Std. Error	2.3	1.1	0.004	0.5
Combined	186.2	88.9	0.228	9.2

Sample ID	500 ppm Al	(Combined)
Operator ID	cjm	
Elapsed Time	00:09:00	
Median Diam.	186.2 nm	
Mean Diam.	206.3 nm	
Polydispersity	0.228	
GSD	1.574	

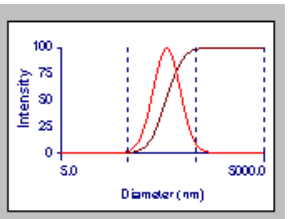

d(nm)	G(d)	C(d)	d(nm)	G(d)	C(d)	d(nm)	G(d)	C(d)
88.3	26	5	166.0	97	40	252.7	80	75
104.1	44	10	175.9	99	45	272.7	70	80
116.4	58	15	186.2	100	50	297.8	58	85
127.1	70	20	197.1	99	55	333.0	44	90
137.2	80	25	208.8	97	60	392.5	26	95
146.8	87	30	221.7	93	65			
156.4	93	35	236.1	87	70			

Intensity

Copy for Spreadsheet

Sample ID	500 ppm Al	(Combined)
Operator ID	cjm	
Elapsed Time	00:09:00	
Mean Diam.	239.1 nm	
Rel. Var.	0.171	
Skew	-0.710	

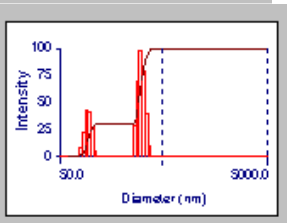

d(nm)	G(d)	C(d)	d(nm)	G(d)	C(d)	d(nm)	G(d)	C(d)
62.4	0	0	124.4	0	31	248.1	0	31
66.5	0	0	132.5	0	31	264.1	28	37
70.8	0	0	141.1	0	31	281.2	70	52
75.3	0	0	150.2	0	31	299.4	100	73
80.2	8	2	159.9	0	31	318.8	81	90
85.4	22	6	170.3	0	31	339.4	40	98
90.9	43	16	181.3	0	31	361.4	9	100
96.8	41	24	193.0	0	31	384.8	0	100
103.1	27	30	205.5	0	31	409.7	0	100
109.8	4	31	218.8	0	31	436.2	0	100
116.9	0	31	233.0	0	31	464.5	0	100

Intensity

high purity water (Combined)

Effective Diameter: 0.0 nm
Polydispersity: 0.000
Avg. Count Rate: 539.7 cps
Baseline Index: 4.3
Time Remaining: 00:07:22

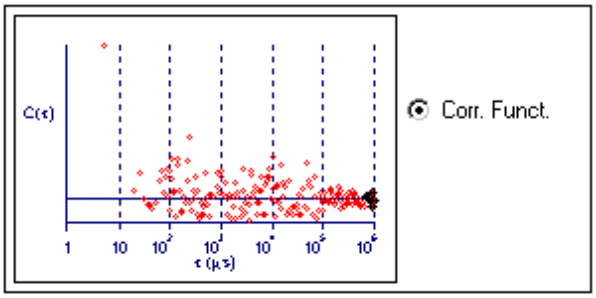

Run	Eff. Diam. (nm)	Half Width (nm)	Polydispersity	Baseline Index
1	0.0	0.0	0.000	0.0
2	0.0	0.0	0.000	0.0
3				
4				
5				
6				
7				
8				
9				
10				
Mean	0.0	0.0	0.000	0.0
Std. Error	0.0	0.0	0.000	0.0
Combined	0.0	0.0	0.000	4.1